FISEVIER

Contents lists available at ScienceDirect

Remote Sensing of Environment

journal homepage: www.elsevier.com/locate/rse



Pantropical modelling of canopy functional traits using Sentinel-2 remote sensing data



Jesús Aguirre-Gutiérrez^{a,b,*}, Sami Rifai^a, Alexander Shenkin^a, Imma Oliveras^a, Lisa Patrick Bentley^c, Martin Svátek^d, Cécile A.J. Girardin^a, Sabine Both^e, Terhi Riutta^{a,aa}, Erika Berenguer^a, W. Daniel Kissling^f, David Bauman^{a,g}, Nicolas Raab^a, Sam Moore^a, William Farfan-Rios^{h,i,j}, Axa Emanuelle Simões Figueiredo^k, Simone Matias Reis^{a,l}, Josué Edzang Ndong^m, Fidèle Evouna Ondo^m, Natacha N'ssi Bengoneⁿ, Vianet Mihindouⁿ, Marina Maria Moraes de Seixas^o, Stephen Adu-Bredu^p, Katharine Abernethy^{q,r}, Gregory P. Asner^s, Jos Barlow^{t,u}, David F.R.P. Burslem^v, David A. Coomes^w, Lucas A. Cernusak^x, Greta C. Dargie^y, Brian J. Enquist^z, Robert M. Ewers^{aa}, Joice Ferreira^u, Kathryn J. Jeffery^r, Carlos A. Joly^{ab}, Simon L. Lewis^{y,ac}, Ben Hur Marimon-Junior^l, Roberta E. Martin^s, Paulo S. Morandi^l, Oliver L. Phillips^y, Carlos A. Quesada^{ad}, Norma Salinas^{a,ae}, Beatriz Schwantes Marimon^l, Miles Silman^{af}, Yit Arn Teh^{ag}, Lee J.T. White^{n,q,r}, Yadvinder Malhi^a

- ^a Environmental Change Institute, School of Geography and the Environment, University of Oxford, Oxford, UK
- b Biodiversity Dynamics, Naturalis Biodiversity Center, Leiden, the Netherlands
- ^c Department of Biology, Sonoma State University, 1801 East Cotati Avenue, Rohnert Park, CA 94928, USA
- d Department of Forest Botany, Dendrology and Geobiocoenology, Faculty of Forestry and Wood Technology, Mendel University in Brno, Brno, Czech Republic
- e Environmental and Rural Science, University of New England, Armidale, 2351, NSW, Australia
- f Institute for Biodiversity and Ecosystem Dynamics (IBED), University of Amsterdam, Amsterdam, the Netherlands
- g Laboratoire d'Écologie Végétale et Biogéochimie, CP 244, Université Libre de Bruxelles, Brussels, Belgium
- ^h Living Earth Collaborative, Washington University in Saint Louis, St. Louis, MO, USA
- ¹ Center for Conservation and Sustainable Development, Missouri Botanical Garden, St. Louis, MO, USA
- ^j Herbario Vargas (CUZ), Escuela Profesional de Biología, Universidad Nacional de San Antonio Abad del Cusco, Cusco, Peru
- k National Institute of Amazonian Research INPA C.P. 2223 69080-971 Manaus AM Brazil
- ¹Laboratório de Ecologia Vegetal (LABEV), Universidade do Estado de Mato Grosso, Nova Xavantina, Brazil
- ^m Agence Nationale des Parcs Nationaux, BP20379, Libreville, Gabon
- ⁿ Ministère des Eaux, des Forêts, de la Mer et de L'Environnement, Libreville, Gabon
- ° Embrapa Amazônia Oriental, Trav. Dr. Enéas Pinheiro, s/n, CP 48, 66095-100 Belém, PA, Brazil
- ^p CSIR-Forestry Research Institute of Ghana, University P.O. Box 63, Kumasi, Ghana
- ^q Institut de Recherche en Écologie Tropicale, Libreville, Gabon.
- ^r Biological and Environmental Sciences, University of Stirling, Stirling, UK.
- s Center for Global Discovery and Conservation Science, Arizona State University, Tempe, AZ, United States
- ^t Lancaster Environment Centre, Lancaster University, Lancaster LA1 4YQ, UK
- ^u MCT/Museu Paraense Emílio Goeldi, Av. Magalhães Barata 376, São Braz, 66040-170 Belém, PA, Brazil
- v School of Biological Sciences, University of Aberdeen, Aberdeen, UK
- [™] Conservation Research Institute, Department of Plant Sciences, University of Cambridge, Cambridge CB2 3QZ, UK
- Conservation Research Institute, Department of Plant Sciences, University of Cambridge,
 College of Science and Engineering, James Cook University, Cairns, Qld 4878, Australia
- y Ecology and Global Change, School of Geography, University of Leeds, Leeds, West Yorkshire, UK
- ² Department of Ecology and Evolutionary Biology, University of Arizona, Tucson, AZ, USA
- aa Department of Life Sciences, Imperial College London, Ascot, UK
- ab Universidade Estadual de Campinas, Instituto de Biologia, Departamento de Biologia Vegetal, Campinas, São Paulo, Brazil
- ^{ac} Department of Geography, University College London, London, UK
- ^{ad} Coordenação de Dinâmica Ambiental, Instituto Nacional de Pesquisas da Amazônia, Manaus, Brazil
- ^{ae} Sección Química, Pontificia Universidad Católica del Perú, Avenida Universitaria 1801, San Miguel, Lima 32, Peru
- ^{af} Department of Biology, Wake Forest University, Winston-Salem, NC 27109, USA
- $^{
 m ag}$ School of Natural and Environmental Sciences, Newcastle University, Newcastle Upon Tyne, UK

^{*}Corresponding author at: Environmental Change Institute, School of Geography and the Environment, University of Oxford, Oxford, UK. E-mail address: jesus.aguirregutierrez@ouce.ox.ac.uk (J. Aguirre-Gutiérrez).

ARTICLE INFO

Keywords:
Plant traits
Sentinel-2
Tropical forests
Random Forest
Pixel-level predictions
Image texture

ABSTRACT

Tropical forest ecosystems are undergoing rapid transformation as a result of changing environmental conditions and direct human impacts. However, we cannot adequately understand, monitor or simulate tropical ecosystem responses to environmental changes without capturing the high diversity of plant functional characteristics in the species-rich tropics. Failure to do so can oversimplify our understanding of ecosystems responses to environmental disturbances. Innovative methods and data products are needed to track changes in functional trait composition in tropical forest ecosystems through time and space. This study aimed to track key functional traits by coupling Sentinel-2 derived variables with a unique data set of precisely located in-situ measurements of canopy functional traits collected from 2434 individual trees across the tropics using a standardised methodology. The functional traits and vegetation censuses were collected from 47 field plots in the countries of Australia, Brazil, Peru, Gabon, Ghana, and Malaysia, which span the four tropical continents. The spatial positions of individual trees above 10 cm diameter at breast height (DBH) were mapped and their canopy size and shape recorded. Using geo-located tree canopy size and shape data, community-level trait values were estimated at the same spatial resolution as Sentinel-2 imagery (i.e. 10 m pixels). We then used the Geographic Random Forest (GRF) to model and predict functional traits across our plots. We demonstrate that key plant functional traits can be accurately predicted across the tropicsusing the high spatial and spectral resolution of Sentinel-2 imagery in conjunction with climatic and soil information. Image textural parameters were found to be key components of remote sensing information for predicting functional traits across tropical forests and woody savannas. Leaf thickness ($R^2 = 0.52$) obtained the highest prediction accuracy among the morphological and structural traits and leaf carbon content ($R^2 = 0.70$) and maximum rates of photosynthesis ($R^2 = 0.67$) obtained the highest prediction accuracy for leaf chemistry and photosynthesis related traits, respectively. Overall, the highest prediction accuracy was obtained for leaf chemistry and photosynthetic traits in comparison to morphological and structural traits. Our approach offers new opportunities for mapping, monitoring and understanding biodiversity and ecosystem change in the most species-rich ecosystems on Earth.

1. Introduction

Some of the most urgent questions in ecology and ecosystem science today focus on how communities of organisms respond to global environmental changes (Naeem et al., 2009), how biodiversity and ecosystem changes across the world can be consistently mapped and monitored (Navarro et al., 2017), and how spatial, temporal and taxonomic variability in biodiversity influences ecosystem resilience to climate change (Oliver et al., 2015). In terms of Earth system science, we need to understand and model how the terrestrial biosphere will respond (and already is responding) to global environmental change, and whether there are critical thresholds or "tipping points" beyond which major biomes may not be able to recover. Nowhere is the challenge more urgent than in the species-rich tropical forest and woody savanna biomes, which together are home to more than half of global biodiversity and over 60% of terrestrial productivity (Beer et al., 2010). There is evidence that atmospheric change may have effects on tropical forest productivity and tree functional composition (Esquivel-Muelbert et al., 2019; Hubau et al., 2020). These effects may include a stimulation of productivity (perhaps due to rising CO2) and/or a degradation or dieback, possibly caused by increased seasonality and incurred intensity of extreme drought events (Malhi et al., 2008; Malhi et al., 2018). Such events are partly responsible for the increased tree mortality and decreased carbon residence time in tropical forests worldwide (McDowell et al., 2018). However, to adequately understand such responses we need to capture and map the high diversity of plant ecosystem function in the species-rich tropics and savannas.

Species functional traits are defined as the morphological, physiological or phenological attributes which determine the fitness of organisms, their response to changes in the environment and their influence on ecosystem functions (Kissling et al., 2018; Díaz and Cabido, 2001). Functional traits provide tangible and mechanistic means of assessing the ability of communities to adapt to climate change (Pacifici et al., 2015) and play a major role in determining ecosystem productivity, functioning and notably nature's contribution to people (e.g. water and wood availability) (Díaz et al., 2019; Carmona et al., 2016). Any tools or methods that facilitate quantification of functional traits across large spatial scales and at high spatial resolution would be invaluable for quantifying ecosystem functioning and ecological

responses to disturbance at scales relevant for policy and management (Kissling et al., 2018). However, it is still challenging to map functional trait diversity in tropical regions given the lack of plant trait data available for most of those locations (Jetz et al., 2016). Additional challenges come from different and often incompatible trait collection protocols and the lack of systematic high spatial, spectral and temporal resolution remote sensing imagery that coincides with data for functional traits at the canopy level and the lack of geo-located tree stems at the plot level. Thus, there is a need for spatially-explicit methods to map and quantify plant functional traits at high spatial resolution in tropical forest and woody savanna ecosystems.

Tracking functional traits can shed light on differences in ecosystem functioning across broad spatial extents and therefore aid policy and decision making, e.g. for creating adequate biodiversity conservation policies or for providing early warning of directional shifts in ecosystems. The key challenges of any functional trait approach are scalability and monitoring: how can functional shifts in highly diverse tropical forests and woody savannas be monitored and tracked over large spatial extents? Intensive field sampling of plant functional traits at a pantropical scale is time-consuming and economically unviable. There are large gaps in the availability of plant trait data globally, and the largest gaps are in the tropics (Jetz et al., 2016). Large plant trait datasets aim to overcome this issue and have advanced our ability to carry out plant functional trait analysis in an unprecedented way (Kattge et al., 2020; Gallagher et al., 2020). However, as with any database, the plant trait values from such databases will represent the local trait-environment relationships for the site where they were collected, which may not be the area of interest. A key assumption in trait-based ecology is that the environment is filtering for an optimal set of trait characteristics so that the resulting communities are adapted to the environment where they are distributed (Fell and Ogle, 2018; Lebrija-Trejos et al., 2010; Lortie et al., 2004). Hence, we might expect an optimal set of trait characteristics for a given location, which when analysed over time could quantify the dynamics of community trait distributions or shifts in functional composition relating to environmental changes (Enquist et al., 2015).

Recently, there has been an increasing investment into mapping plant functional trait distributions given economic and data availability constraints such efforts have mostly focused on hyperspectral imagery at local (Schneider et al., 2017) to regional scales (Asner et al., 2015; Asner et al., 2016). However, high resolution hyperspectral imagery is not widely available (Clark, 2017; Szabó et al., 2019). Landsat-8 imagery at coarser spatial (30 m pixel), spectral and temporal resolution than Sentinel-2 imagery has been used to map four traits over small (20 × 20 m) vegetation plots covering small spatial extents (Wallis et al., 2019). The spatial mismatch between site-level trait sampling and the spatial resolution of pixels may partly affect overall model predictions (Wallis et al., 2019). Other studies restricted to European forests (Ma et al., 2019) show how Sentinel-2 imagery could be used to map functional trait diversity in the comparatively low tree diversity forests of Europe (Ma et al., 2019) and to retrieve specific leaf area from Landsat-8 imagery (Ali et al., 2017). However, the tropics present a different set of challenges, such as the high species richness, low accessibility and comparatively low availability of trait data, plus the low coverage of remote sensing data because of persistent high cloud cover. These challenges have hampered developments in mapping plant functional trait distributions across most tropical areas.

Satellite imagery with high spectral, spatial and temporal resolution

is particularly needed in the wet tropics (Asner et al., 2017), where clear days can be infrequent and several images may be required to construct a cloud-free composite. The Copernicus mission from the European Space Agency's (ESA; www.esa.int) aids in the improvement in this area. The Sentinel-2 multispectral imager satellites are part of the Copernicus programme, which has the potential to provide new opportunities to evaluate canopy traits remotely. Sentinel-2 has 13 spectral channels covering the visible, near-infrared, and short-wave infrared, a spatial resolution of 10 m for visible and near-infrared, 20 m for short-wave infrared, revisit period of 5 days and it provides open data availability. The improved spectral sampling (13 bands, 10 excluding the 60 m atmospheric bands) and fine spatial resolution of the Sentinel-2 images have the potential to elucidate leaf chemistry, morphology, photosynthesis and water content at the pixel-level, although this remains largely untested. Multispectral sensors do not provide the rich information available from hyperspectral sensors, which have been used in numerous studies to map functional traits at small spatial extents (Townsend et al., 2003; Laurin et al., 2016; Asner et al., 2015; Martin et al., 2008). However, high resolution open-access

Table 1
Collection details for vegetation plots and plant functional traits. A total of 2434 individual trees were sampled for functional traits.

Location	Species sampled for traits	Plot code	Size (ha)	Centroid coo	rdinates	Date of collection			
				X	Y	Vegetation census	Traits		
Australia	60	AEP-02	0.5	145.586	-17.146	2011	June–September 2015		
		AEP-03	0.5	145.592	-17.088				
		DRO-01	0.9	145.430	-16.103				
		ROB-06	1	145.630	-17.121				
Ghana	63	ANK-01	1	-2.696	5.268	2013	October-March 2015/2016gramm		
		ANK-03	1	-2.692	5.271				
		BOB-01	1	-1.339	6.691	2015			
		BOB-02	1	-1.319	6.704				
Gabon	41	LPG-01	1	11.574	-0.174	2014	February–March 2017		
		LPG-02	1	11.615	-0.216				
		MNG-04	1	9.324	0.577	2016			
Brazil -NX	64	NXV-01	1	-52.352	-14.708	2015	March-May 2014		
		NXV-02	1	-52.351	-14.701		15 14 February–March 2017 16 15 March–May 2014 14 14 August–September 2015 13 April–November 2013		
		VCR-02	1	-52.168	-14.832				
		NXV-10-1	0.1	-52.353	-14.713	2014			
		NXV-10-2	0.1	-52.352	-14.713				
		NXV-10-3	0.1	-52.351	-14.713				
		NXV-10-4	0.1	-52.349	-14.713				
		NXV-10-5	0.1	-52.346	-14.713				
		NXV-10-6	0.1	-52.349	-14.712				
		NXV-10-7	0.1	-52.348	-14.711				
		NXV-10-8	0.1	-52.347	-14.711				
		NXV-10-9	0.1	-52.347	-14.711				
		NXV-10-10	0.1	-52.346	-14.712				
Brazil -ST	136	261-10	0.25	-55.005	-3.019	2014	August-September 2015		
		261-9	0.25	-55.015	-3.040		0		
		363-6	0.25	-54.956	-3.337				
		363–3	0.25	-54.963	-3.297				
		363–7	0.25	-54.961	-3.321				
Peru	159	ESP-01	1	-71.595	-13.176	2013	April-November 2013		
		PAN-02	1	-71.263	-12.650				
		SPD-01	1	-71.542	-13.047				
		SPD-02	1	-71.537	-13.049				
		TRU-04	1	-71.589	-13.106				
		WAY-01	1	-71.587	-13.191				
		ACJ-01	1	-71.632	-13.147	2014			
		PAN-03	1	-71.274	-12.638				
		TAM-05	1	-69.271	-12.830				
		TAM-06	1	-69.296	-12.839				
Malaysia	283	SAF-01	1	4.732	117.619	2016	July-December 2015		
,		SAF-02	1	4.739	117.617	====			
		SAF-03	1	4.691	117.588				
		SAF-04	1	4.765	117.700				
		DAN-04	1	4.951	117.796				
		DAN-05	1	4.953	117.793				
		MLA-01	1	4.747	116.970				
		MLA-02	1	4.754	116.950				

Brazil -NX: Nova Xavantina; Brazil -ST: Santarem; Malaysia: Malaysian Borneo.

 Table 2

 Description of plant functional traits collected across the tropics and their relevance under a changing environment.

Description of plant tune	cuonal uans c	ollected actoss i	Description of piant functional traits confected across the hopics and then relevance under a changing environment.	nanging environment.	
Trait	Abbreviation	Units	Description	Relevance	References**
Leaf area	Area	cm^2	One-sided area of the leaf	Higher leaf area could result in higher levels of light capture and photosynthetic activity.	(Walker et al., 2014, Wright et al., 2004, Juneau and Tarasoff, 2012, Díaz et al., 2016, Hawthorne, 1995, Chave
Specific leaf area	SLA	$m^2 g^{-1}$	One-sided area of a leaf divided by dry mass	Relevant for photosynthetic capacity, light capture, water loss, net assimilation rate, leaf life span.	et al., 2006, Huang et al., 2019)
Leaf thickness	Thickness	шш	Thickness of a fresh leaf	Trade-off between decreasing water transpiration at the expense of higher construction investment and probably lower photosynthetic efficiency in thicker leaves.	
Leaf nitrogen content	z	%	Content per unit dry leaf mass	Nutrient relevant for metabolic reactions, including light capture, related	
Leaf phosphorus content	Ь	%		to photosynthetic capacity and growth. Restricted availability of some	
Leaf carbon content	C	%		nutrients may limit plant carbon acquisition and growth.	
Leaf calcium content	Ca	%			
Leaf potassium content	Ж	%			
Leaf magnesium content	Mg	%			
Leaf water content	LWC	%	Amount of water in the leaf relative to its	Leaf mass is a proxy of leaf biomass investment which may vary	
	í		dry and fresh mass	depending on environmental conditions and phenology of species. It has	
Leaf frash mass	Dry mass	b0 b	Mass of a dry leaf	been considered relevant for photosynthetic potential.	
Amax	Amax	μ mol m ⁻² s ⁻¹	Light-saturated maximum rates of net	Indicate the maximum CO ₂ assimilation and are thus indices of leaf	
			photosynthesis at saturated CO_2 (2000 ppm CO_2)	photosynthetic capacity	
Asat	Asat	s m lomi	Light-saturated rates of net photosynthesis at ambient CO ₂ concentration (2000 ppm CO ₂)		

* References are not exhaustive.

hyperspectral imagery is not currently available from space. Although Landsat images have been used to predict a few functional traits at a local scale (Wallis et al., 2019), the extended spectral, spatial and temporal capabilities of the state-of-the-art sensors onboard the Sentinel-2 satellites provide greater potential for mapping functional trait diversity in tropical forest ecosystems at large extents.

Here, we employ a unique and large dataset of in-situ plant canopy traits and vegetation census data collected with a standardised protocol at multiple sites across the tropics to calibrate and validate Sentinel-2 imagery for predicting community leaf trait composition. The data provide 14 standardised measurements of in-situ collected plant functional traits, precisely geo-located and delineated individual tree crowns and vegetation censuses from Australia, South East Asia, Africa and South America to model and predict functional trait composition at the pixel-level. We investigate how functional traits of tropical forests vary within and between these different tropical regions and whether Sentinel-2 spectral data in conjunction with climatic and soil information provide sufficient information to predict such pixel-level trait composition in long-term vegetation plots across the tropics. We hypothesised that there would be differences in trait variation among sites and regions given the range of climatic and soil conditions across the tropics. Given the high spectral and spatial resolution of Sentinel-2 imagery we further hypothesised that raw spectral bands and textural information will prove to be key predictors of functional trait distributions across the tropics. The very high spatial resolution and local origin of the input plant traits and census dataset, which represent traits adapted to local environments, plus the use of the Sentinel-2 data will allow us to accurately predict plant functional trait distributions that are potentially generalisable across the tropical forest biome.

2. Methods

2.1. Vegetation plots

We collected vegetation census data from 47 permanent vegetation plots that are part of the Global Ecosystems Monitoring network (GEM; www.gem.tropicalforests.ox.ac.uk). These plots encompass wet tropical forests, seasonally dry tropical forests, and tropical forest-savanna transitional vegetation. The sampled vegetation plots have an area ranging from 0.1 to 1 ha, with most (61%) being 1 ha. The plots used are located across four tropical continents and specifically in the countries of Australia, Brazil, Gabon, Ghana, Malaysian Borneo (from here onwards referred to as Malaysia) and Peru (Table 1). In each plot all woody plant individuals with a diameter \geq 10 cm at breast height (DBH) or above buttress roots were measured and their exact geographic location was recorded (see the 'Individual tree crowns' section below for more details). In two plots (NXV-01 and NXV-10) in Nova Xavantina, here onwards referred to as Brazil-NX, the DBH was measured near ground level as is standard in savanna monitoring protocols.

2.2. Functional traits

We collected plant functional trait measurements from all woody plants located in each of the 47 vegetation plots mentioned above (Table 2). All traits were gathered from the GEM network and were collected following a standardised methodology across plots. Forest inventory data were used to stratify tree species by basal area dominance, a proxy for canopy area dominance. The tree species that contributed most to basal area abundance were sampled with 3–5 replicate individuals per species, with a goal of sampling 60–80% of basal area across the sampling region. Eighty percent of basal area was often achieved in low diversity sites (e.g. montane or dry forests) but only around 60% was achieved in some high diversity sites (lowland humid rainforests). For each selected tree a sun and a shade branch were sampled and in each branch 3–5 leaves were used for trait measurements. We only included the sun exposed branches in our analysis

because we were interested in the branches that could potentially be receiving direct sun radiation and thus show direct spectral reflectance. This represented a total sample of 2434 individual trees across the tropics (Table 1). The plant functional traits collected were those related to photosynthetic capacity at both saturating CO2 concentration (2000 ppm CO₂; A_{max}) and ambient CO₂ concentration (400 ppm CO₂; A_{sat}); leaf chemistry (nitrogen, phosphorus, carbon, calcium, potassium and magnesium content); and leaf morphological and structural traits (area, specific leaf area, thickness, dry mass, fresh mass and water content). An overview of the methods for individual leaf functional trait measurements is provided in the Supplementary Information (see full traits collection protocol section). Further details of measurements for the Peruvian Andes campaign are given in Martin et al. (2020) and Enquist et al. (2017), for the Malaysian campaign in Both et al. (2019), and for the Ghana and Brazil campaigns in Oliveras et al. (2020) and Gvozdevaite et al. (2018).

Some individuals in the plots lacked functional trait values. To assign representative trait values to unsampled individuals we did the following: 1) individuals from which traits were measured kept their original trait information, 2) for individuals with no trait information we randomly sampled trait values from other individuals from the same species present in the same plot, 3) if the species was not sampled in the given plot then we randomly sampled an individual from the same species that had trait information in other plots from the same region (Table 1). This protocol for trait value allocation allowed us to work with the existing range of trait values at the species level and avoided to create average values per species (Cadotte et al., 2011; Schneider et al., 2017). We did not assign trait values to the remaining individuals belonging to species from which no trait collection was obtained at the regional level.

2.3. Individual tree crowns

Tree crown locations and structural attributes were recorded for each tree, where crown area and shape were measured by direct crown field measurements in the case of plots in Malaysia and Peru (see protocol below), or by means of regional level allometric equations developed by Shenkin et al. (2019) (all other plots). In the latter case, the crown's shape was assumed to be circular. The direct field crown measurements were as follows: all trees ≥ 10 cm DBH (i.e., 1.3 m from the ground) were mapped using a ground-based Field-Map laser technology (IFER, Ltd., Jílové u Prahy, Czech Republic) (Hédl et al., 2009). The Field-Map technology was based on a combination of Impulse 200 Standard laser rangefinder (with in-built tilt sensor for measuring vertical angles), MapStar module II electronic compass (both Laser Technology Inc., Colorado, USA), and the specialized mapping software Field-Map v. 11 (IFER, Czech Republic). The technology was used to record spatial positions of tree stems in three-dimensional space (x, y, zcoordinates) as well as to map individual horizontal projections of tree crowns in the plots. The horizontal crown projection of every tree was obtained by measuring spatial positions (x and y-coordinates) of series of points (ranging from 5 to 30 points depending on the size of the crown) at the boundary of a crown projected to the horizontal plane. The shape of crown projection was subsequently smoothed using the "smooth contour line" feature of Field-Map software v. 11. Heights of all trees with DBH \geq 10 cm were measured by the Impulse and Tru-Pulse 360 R laser rangefinders (both Laser Technology Inc., Colorado, USA). Thus, each individual crown was accurately geolocated rendering information about its shape and vertical and horizontal position.

2.4. Calculating pixel-level trait composition

We calculated the community weighted mean of each trait for each 10×10 m subplot (matching the highest pixel spatial resolution of the Sentinel-2 imagery) based on the mass ratio hypothesis, which states that the most dominant species drive the ecosystem processes by means

of their functional traits (Grime, 1998). We first geolocated the vegetation plot, with its already mapped tree crowns (see protocol above), to the Sentinel-2 imagery based on the corner coordinates of the plots.

This is an important step as geolocation errors between the vegetation plot and the correct location in the satellite image could represent a large proportion of a given plot depending on the plots' area. Then for

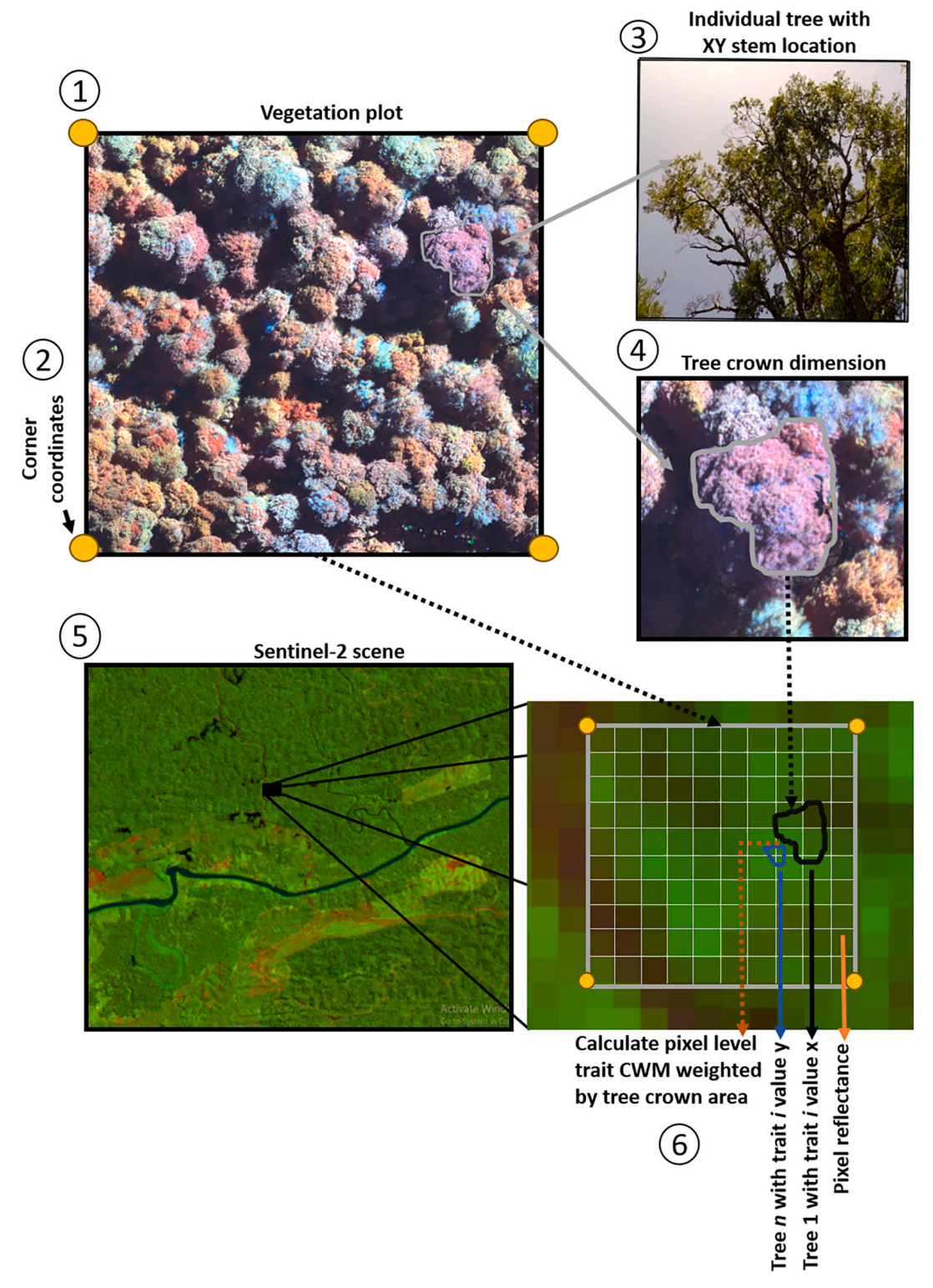


Fig. 1. Diagram summarising the steps followed to assign trait values per Sentinel-2 pixel. 1) First the vegetation plots are defined based on the GEM (Global Environmental Monitoring) dataset and 2) from each vegetation plot the corner coordinates are extracted. 3) From each vegetation plot the XY position of each stem ≥ 10 cm DBH is extracted and 4) the crown horizontal area is calculated based on the protocol described in the methods section. 5) Then the Sentinel-2 imagery for the study area is processed to level 2A using the ESA SNAP toolbox and 6) the vegetation plot is overlaid in the Sentinel-2 image based on its corner coordinates. In this last step (6) each pixel defines a 'subplot' which is the unit used to calculate the trait community weighted mean based on the crown area of the trees that are contained by that pixel. In 6) n refers to a given tree in a given pixel, trait i represents a given trait and x and y are values for that trait. The image used as an example in step (1) was taken by Jesus Aguirre-Gutierrez over a vegetation plot using a multispectral ALTUM camera mounted on an Inspire 1 drone."

each of the traits, t, and pixels, p, we calculated their community level weighted mean (CWM) using the individual tree crown horizontal area as the weighting factor (Fig. 1) as follows:

$$CWM_{tp} = \frac{\sum_{i=1}^{N} CA_{ip} \times t_{ip}}{CA_{p}} \tag{1}$$

Where CA_{ip} is the crown area of individual i in pixel p, t_{ip} is the trait value of individual i in pixel p, N is the total number of individuals per pixel and CA_p is the crown area of pixel p. The crown contribution to the CWM was weighted by its proportional cover of the corresponding pixel. The total number of pixels used in our calculations are 403 for Australia, 449 for Brazil -NX (Nova Xavantina), 302 for Brazil -ST (Santarem), 464 for Gabon, 620 for Ghana, 976 for Malaysia and 1280 for Peru.

2.5. Sentinel-2 data, vegetation indices and canopy texture parameters

We gathered Sentinel-2 imagery that was closest in time and season to the sampling dates of functional traits and vegetation census across the tropics for each of the study locations (Table S1). The Sentinel-2 imagery was first selected using the European Space Agency (ESA) ScienceHub choosing images with high pixel quality and low cloud cover (< 10%). Atmospheric, radiometric and topographic corrections were applied to the selected imagery (Level 1C) using the Sen2Cor algorithm in the Sentinel SNAP toolbox (step.esa.int). Our overlapping imagery with the vegetation plots appeared free of clouds and cirrus effects. The above-mentioned steps allowed us to obtain level 2A imagery with surface reflectance values. We then resampled the 20 m bands to 10 m spatial resolution using bilinear interpolation. The Sentinel-2 60 m resolution bands (B01, B09, B10) were not used as these are designed for cirrus, water vapour and cloud detection (Table 3). Band 8A was not used as it covers an overlapping spectral window with band 8 and has a lower spatial resolution. Since vegetation indices may increase prediction accuracy when modelling community weighted traits (Wallis et al., 2019), we calculated three of them (Table 3) which we hypothesised to inform trait distributions given their association with chlorophyll and nutrient levels in the leaves and their use of the visibleto-red edge spectral bands.

Canopy structure may play an important role in separating different vegetation types and differences in canopy spectral composition. To characterise canopy structure, we calculated the Grey Level Co-Occurrence Matrix (GLCM) based texture features (Haralick et al.,

1973). The desired texture metrics are computed from a grey tone matrix that is spatially dependent. The co-occurrence matrix depends on the angular relationship and distance between two neighbouring pixels and depicts the number of occurrences of the relationship between a pixel and its neighbour. After trials with smaller windows size (5×5) we opted to use a 9×9 pixel kernel window which was sufficient to render enough canopy contrast information during the modelling step (see section 2.7 below) without taking large periods of time for its calculation. The texture results obtained with the used kernel window was highly correlated to the smaller kernel window (Cor = 0.94, $P \le 0.0001$). Based on the GLCM we calculated two variables that are least correlated with each other, the Entropy and Correlation, for each of the vegetation indices. While Entropy measures the homogeneity level for a given area, the Correlation measures probability of occurrence of the specified pixel pairs across the image (Haralick et al., 1973; Wallis et al., 2019). All remote sensing analyses related to the generation of vegetation indices and texture metrics were carried out using the Sentinel SNAP toolbox (step.esa.int) and the R statistical environment (R Development Core Team, 2014) with the 'Sen2R' package.

2.6. Environmental and soil data

Climatic, topographic and soil characteristics may vary across regions and could at least partly determine the region's vegetation and intrinsic trait composition. We obtained information on these three components for each sampling location. The three components were grouped as belonging to environmental (climate) or soil-terrain (texture, pH, cation exchange capacity and topography) drivers (Table 3).

For climate and for each sampling location we gathered gridded data on the mean annual climatic water deficit (MCWD), which is a metric of drought intensity and severity, mean annual maximum temperature (MATmax), solar radiation (SRAD) and soil moisture (SM) (Table 3). All climatic data with a spatial resolution of ~4 km were obtained from the TerraClimate gridded climate product (Abatzoglou et al., 2018). To characterise the climatic conditions for each location we used a climatology of 30 years (1986–2015) as suggested by the World Meteorological Organization (WMO; www.wmo.int/pages/prog/wcp/ccl/faqs.php). We used the terrain slope to characterise the plot's topography, as it has been shown that topography may shape the composition and structure of tropical forests (Jucker et al., 2018) and may affect the vegetation spectral reflectance by modifying soil water

Table 3
Spectral remote sensing, environmental and soil related variables used during the modelling protocol. All climatic variables but slope were calculated using a climatology of 30 years (1986–2015). All soil variables were calculated for the top 30 cm soil layer. Sentinel-2 band wavelengths (nm) are given in parenthesis after the band name.

Type	Variable	Description	References
RS	B2 (490), B3 (560), B4 (665), B8 (842)	Sentinel-2 bands with spatial resolution of	www.esa.int
		10 m	
	B5 (705), B6 (740), B7 (783), B11 (1610),	Sentinel-2 bands with spatial resolution of	
	B12 (2190)	20 m	
	MCARI	Modified Chlorophyll Absorption in	(Daughtry et al., 2000)
		Reflectance Index	
	MSAVI2	Modified Soil Adjusted Vegetation Index 2	(Qi et al., 1994)
	NDRE	Normalized Difference Red edge Index	(Barnes et al., 2000)
	Texture	Entropy, calculated for vegetation indices	(Haralick et al., 1973)
		Correlation, calculated for vegetation indices	
Climate	MCWD	Mean annual climatic water deficit	(Abatzoglou et al., 2018)
	MATmax	Mean maximum annual temperature	
	SM	Soil moisture as a water balance indicator	
	SRAD	Downward Solar Radiation	
Soil-Terrain	eCEC	Cation Exchange Capacity (mmol ⁺ /kg ⁻¹)	Plot level soil data from the Global Environmental Monitoring
	pH	Soil pH (H2O solution)	(GEM) database
	Clay (%)	Amount of clay (weight %)	
	Sand (%)	Amount of sand (weight %)	
	Slope	Terrain slope (30 m resolution)	(Farr et al., 2007)

and nutrient availability. Terrain slope was calculated using a high-resolution digital elevation model, $\sim 30\,\mathrm{m}$ pixel size at the equator, from the Shuttle Topography Mission (Farr et al., 2007). At most sites soil data were sampled locally, and analysed to a standardised protocol in labs in either INPA, Manaus, Brazil or the University of Leeds, UK, following the RAINFOR soil protocol (Quesada et al., 2012). From these data we summarised plot level soil data averaged over the first 30 cm for texture (Sand% and Clay%), cation exchange capacity (eCEC) and pH-H₂O (pH). Plot level texture data were not available for plots in Australia and the NXV-10 plots and were thus derived from the Soil-Grids dataset at 250 m pixel spatial resolution for those plots only (Hengl et al., 2017).

2.7. Comparing community level trait distributions across regions

We tested if and to what extent the community-level trait distributions differed among regions. We square-root transformed the trait value to improve normality and applied an analysis of variance (ANOVA). We then applied a Tukey's Honest Significant Difference (Tukey HSD) test to investigate the significance of the differences between the means of the community weighted mean (CWM) trait values among locations. The ANOVA and Tukey test were carried out using the 'stats' package for R (R Development Core Team, 2014).

2.8. Relating pixel-level trait composition to spectral reflectance, environment and soil conditions

We modelled the community weighted mean (CWM) of each trait at the pixel-level (10 \times 10 m) as a function of the Sentinel-2 remote sensing, environmental and soil covariates (Table 3) using a 'spatial' version of the machine learning Random Forest (RF) algorithm (Breiman, 2001) named Geographic Random Forests (GRF) (Georganos et al., 2019). RF is a nonparametric algorithm that has been shown to be robust to overfitting and variable inputs thanks to the bagging process and its random feature selection (Hastie et al., 2009). Moreover, it has been extensively used to model and predict ecological and remote sensing data within and across ecosystems (e.g. Asner et al., 2016; Van der Plas et al., 2018). In contrast to RF, GRF disaggregates the underlying data in geographic space, in this case based on the spatial coordinates of the Sentinel-2 pixels, building global and local sub-models (plot level), making the modelling framework thus spatially explicit. The explicit inclusion of the spatial component (XY pixel location) in the models, which are sequentially fitted with different sets of the training data (the bagging process) may contribute to the observed reduced spatial autocorrelation of GRF in comparison to the common RF (Georganos et al., 2019). In the GRF, a global model is built as in other RF applications. However, GRF also generates a local RF for each location, which includes a specified number of nearby observations, here defined by all pixels in the vegetation plot (mostly 1 ha; Table 1), called 'neighbourhood', obtaining in this way metrics of local and global model predictive power and variable importance. For model predictions, a fusion between the global model (that uses more data) and local models (with low bias) can be applied, weighting the contributions of the global and local models based on the parameters that increase the predictive accuracy and decrease the model's Root Mean Square Error (RMSE). We used the spatial GRF to fit a global model for each functional trait (first eliminating statistical outliers) and also fit a specific model for each region (Australia, Brazil -ST, Brazil -NX, Gabon, Ghana, Malaysia and Peru) using the SpatialML package in R.

We performed an extensive set of model optimization and regularization procedures to reduce over-fitting. For the CWM models we selected the number of trees to fit by 10-fold cross-validation analysis with number of trees ranging between 500 and 1500 and the number of variables randomly sampled as candidates at each split (mtry) ranging between 1 and 10, using in the final model the combination of terms that generated the lowest RMSE. All covariates included in the models

had pairwise Pearson correlation coefficients $r \le 0.82$ (Table 3). For the final global and local models, we used 80% of the data for model fitting and the remaining 20% for model evaluation. Variable importance for each model was computed as the decrease in node impurities from splitting on the variable, averaged over all trees and derived from the Out of Bag (OOB) error. Then the resulting importance was standardised to a 0–1 scale for comparison purposes.

We carried out all analyses stated above with the full set of tree individuals present in each vegetation plot with functional traits assuming that the contribution of small individuals to the trait CWM value, and thus to the community reflectance at the pixel-level, would be minimal given the weighting factor used (i.e. the individual's crown area). However, to underpin this we carried out all analyses on two smaller datasets, one where the 25th and other where the 50th percentile of the smallest trees per region were removed. All analyses were carried out in the R statistical environment with the 'caret', 'tidyverse' and 'SpatialML' packages. All covariates were centrered and standardized (z-scores) prior to model building.

3. Results

3.1. Variation in trait composition across tropical forests

Most leaf functional traits exhibited significant differences across the tropics (Fig. 2) including wide trait range variation within the same region (Fig. S8), with leaf fresh mass and leaf thickness being on average less variable among locations (Table S2).

Leaf chemistry and photosynthetic capacity (A_{max} and A_{sat}) often showed significant differences among locations (Table S2). Drier locations as in Nova Xavantina (Brazil -NX) displayed trait adaptations to seasonal rainfall and temperature with on average thicker and smaller $(30 \pm 0.05 \,\text{mm} \text{ and } 56.2 \pm 24.7 \,\text{cm}^2 \text{ respectively})$ leaves at the community level, with some of the highest community-level leaf nitrogen concentration (2.2 \pm 0.3%) and highest photosynthetic capacity (mean $A_{max}=21.9\pm4.3\,\mu mol\,m^{-2}\,s^{-1}$, and $A_{sat}=8.3\pm2.5\,\mu mol\,m^{-2}\,s^{-1}$). In contrast, wetter regions such as Malaysia displayed on average some of the biggest (113.5 \pm 55 cm²) and thinnest (0.25 \pm 0.05 mm) leaves with high leaf water content (59.1 \pm 5%). The Peruvian altitudinal transect showed large variation in community-level traits values, which often overlapped with trait values from all other sampled locations across the tropics (Fig. 2). For most nutrients, leaf nutrient concentration was often highest in forests found in Ghana (e.g. K% = 0.97 ± 0.27 and Mg% = 0.33 ± 0.1) and Malaysia (K% = 1.05 \pm 0.27 and Mg% = 0.27 \pm 0.1). Australian forests showed on average some of the lowest community-level N $(1.3 \pm 0.21\%)$ and P $(0.07 \pm 0.01\%)$ leaf concentrations.

3.2. Pantropical and local community level functional trait models

The analyses carried out with the full dataset and the dataset where the 25th and 50th percentile of the smallest trees per region were removed gave similar results for the global ($R^2=0.95$ and $R^2=0.97$ respectively; Table S3) and local ($R^2=0.81$ and $R^2=0.80$ respectively; Table S4) models of plant trait distributions. Therefore, in the following we only present the results for the models carried out with the full vegetation dataset.

The accuracy of the pantropical prediction of functional traits ranged between a minimum of $R^2 = 0.26$, for leaf fresh mass, and a maximum of $R^2 = 0.70$ for leaf carbon content (C%) based on the out-of-sampled (testing) data across the tropics (Table 4). The predictive accuracies of leaf chemistry and photosynthetic traits were often higher than for morphological and structural traits such as leaf dry mass ($R^2 = 0.27$) and leaf area ($R^2 = 0.43$) (Fig. 3). At the pantropical level, the highest prediction accuracy was obtained for leaf thickness ($R^2 = 0.52$) for morphological and structural traits, for leaf Ca (Ca%; $R^2 = 0.64$) and leaf K (K%; $R^2 = 0.63$) for the chemical traits other than

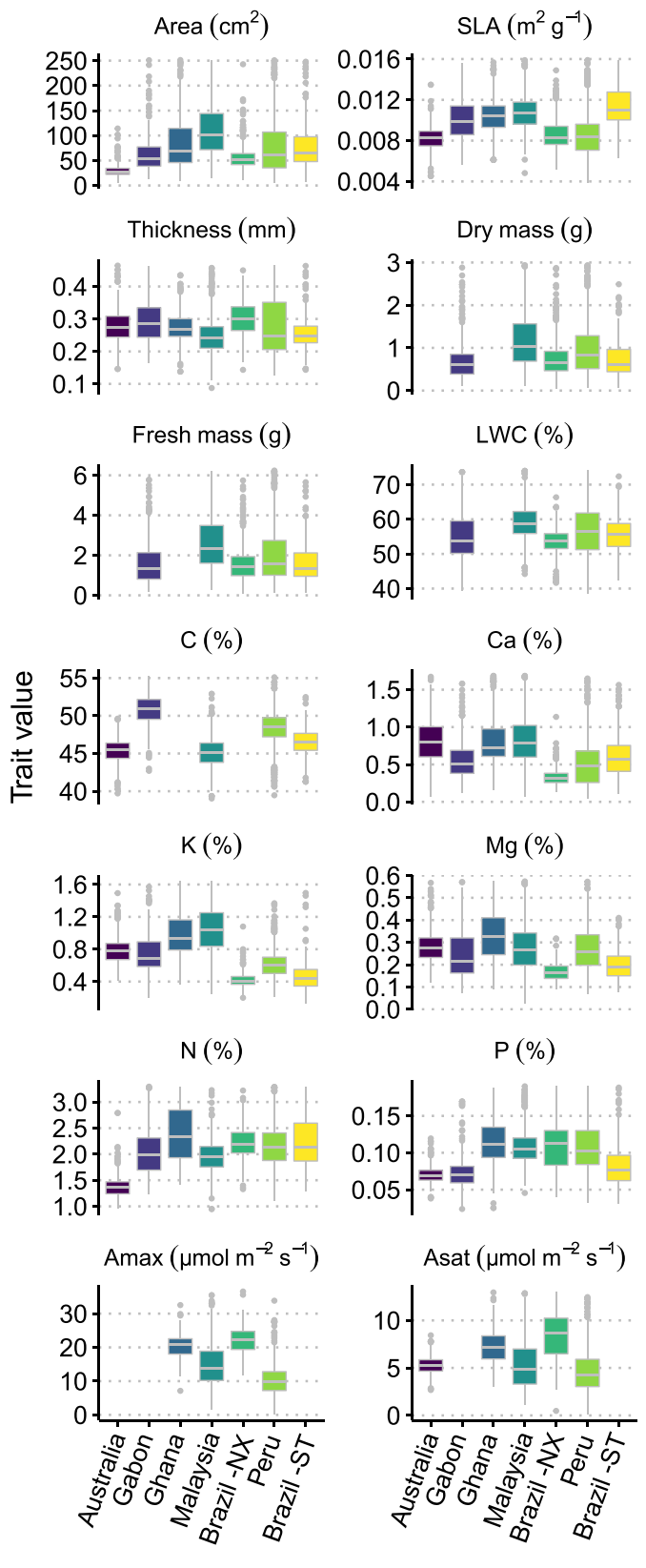


Fig. 2. Comparison of trait distributions across tropical regions. The boxplots are based on the pixel-level ($10 \times 10 \,\mathrm{m}$) community trait values for each trait and region (n=403 for Australia, 449 for Brazil-NX, 302 for Brazil-ST, 464 for Gabon, 620 for Ghana, 976 for Malaysia and 1280 for Peru). Horizontal lines in each boxplot show the median value and vertical lines are the whiskers that extend to the largest value or not further than 1.5 times the inter-quartile range. For some locations information for all traits was not available. For full details in significant differences in mean trait values among locations see Table S4. Brazil -NX: Nova Xavantina; Brazil -ST: Santarem.

Table 4Statistical results on the test data (20% of full dataset) for the global trait distribution models. The prediction accuracy is shown by the R² score.

Туре	Trait	MAE	RMSE	R^2
Morphological and structural	Area (cm ²)	28.32	39.854	0.43
	Dry mass (g)	0.349	0.48	0.27
	Fresh mass (g)	0.799	1.075	0.26
	$SLA (m^2 g^{-1})$	0.001	0.001	0.50
	Thickness (mm)	0.034	0.046	0.52
Chemistry	LWC (%)	3.718	4.886	0.36
	C (%)	1.237	1.615	0.70
	Ca (%)	0.14	0.204	0.64
	K (%)	0.133	0.186	0.63
	Mg (%)	0.055	0.075	0.46
	N (%)	0.23	0.3	0.59
	P (%)	0.015	0.02	0.59
Photosynthetic	Amax $(\mu \text{mol m}^{-2} \text{s}^{-1})$	2.89	3.937	0.67
	Asat $(\mu \text{mol m}^{-2} \text{s}^{-1})$	1.297	1.734	0.55

MAE: Mean Absolute Error; RMSE: Root mean square error.

carbon. Leaf N and P concentrations were also predicted with high accuracy ($R^2=0.59$). Leaf photosynthetic capacity traits, $A_{\rm max}$ and $A_{\rm sat}$, showed some of the highest prediction accuracies ranging from $R^2=0.55$ to 0.67, respectively. Model spatial predictions for several traits and locations are shown in Fig. 4 and others can be seen in Fig. S1-Fig. S7.

Models built for each tropical region and trait uncovered marked differences in prediction accuracy among them (Fig. 5; Table 5 and Table S5). Leaf area prediction accuracy ranged from $R^2 = 0.04$ (Brazil -ST) to 0.35 (Australia), and that of specific leaf area (SLA) ranged from $R^2 = 0.06$ for Malaysia to 0.54 for Brazil -NX (Table S5). The local models showed a higher accuracy for predicting local level leaf chemical nutrients (up to $R^2 = 0.68$), especially for P, Ca, and N concentrations in comparison to morphological (e.g. leaf area and SLA) traits (Table 5; Fig. 5). Traits related to photosynthetic capacity showed an overall better prediction accuracy than leaf area and SLA with prediction values ranging between 0.36 (Peru) to 0.49 (Ghana) for Amax and up to 0.52 for Asat (Brazil -NX; Fig. 5). On average the highest prediction accuracy across regions for a given trait were reached for leaf P concentration ($R^2 = 0.47$) and A_{max} ($R^2 = 0.44$) and the locations with the highest average prediction accuracy across traits were the Nova Xavantina savanna (Brazil -NX, $R^2 = 0.40$) and the Peru elevation gradient ($R^2 = 0.38$; Table 5), both sites encompassing strong gradients in vegetation morphology and structure.

3.3. Importance of spectral remote sensing, climatic and soil data for mapping trait distributions

We included Sentinel-2 band derived reflectance values, vegetation indices, their canopy texture parameters, climatic and soil variables in the general trait models to predict community level traits at the pixellevel (Table 3). The importance of these variables for predicting traits depended on the specific trait being addressed (Fig. 6). In the global model, the remote sensing texture parameters were the first or second major contributor for predicting nine of the functional traits across the tropics (Fig. 6 and Fig. S9). Raw spectral variables were the second most important group for predicting four of such functional traits but often lower in importance than the textural parameters. In the global model, soil and terrain factors were on average some of the most important for predicting photosynthetic traits and foliar P concentration. On average, climatic variables were important for predicting 11 out of 14 functional traits but their contribution was lower for predicting leaf dry and fresh mass and leaf water content (Fig. 6). However, it is evident that a combination of textural, spectral, climatic and soil information is required to obtain the best general model predictions across functional traits and no single variable appears as the most

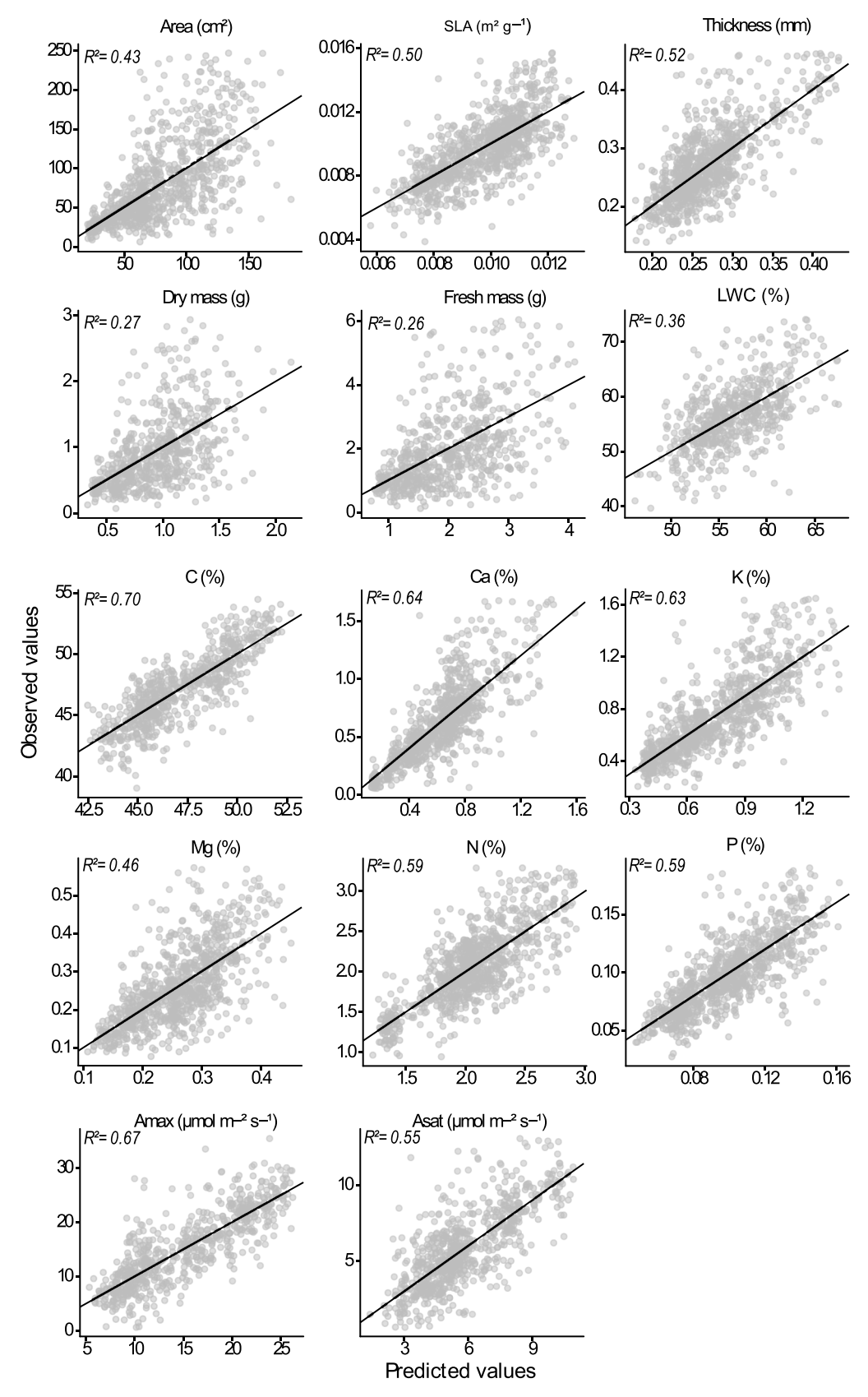
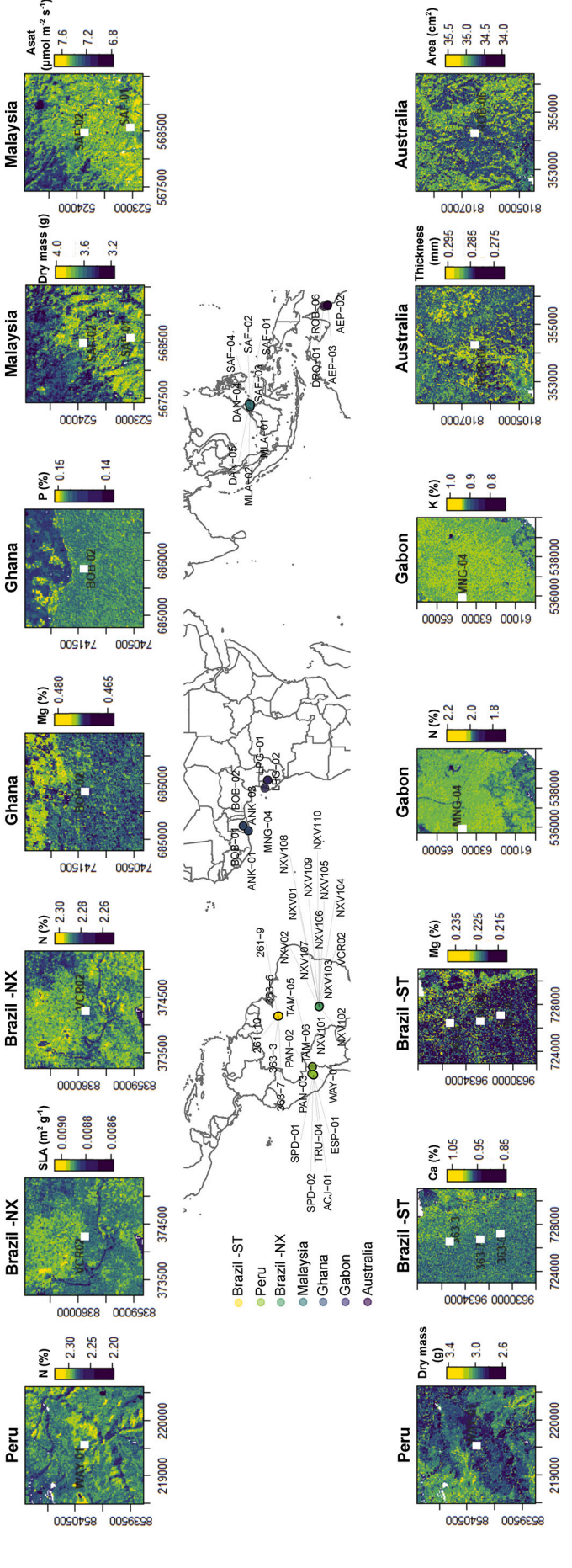


Fig. 3. Model predictions to the 20% test data from the general model which was fitted with 80% of the trait data from across the tropics. Grey dots are the observed against predicted trait values of the pixel-level ($10 \times 10 \, \text{m}$) community weighted mean traits from the test dataset. The black line shows the 1:1 relationship between observed and predicted values. Model prediction accuracy is shown in the top left. Full model results are shown in Table 4.



predictions (top and bottom rows) were obtained using the general models (Table 4) for each of the traits and locations at a 10 × 10 m pixel resolution. The approximated location of each vegetation plot used is shown as 4. Spatial predictions of trait distributions for a selected subset of plant traits and locations. The map (middle) shows the locations of vegetation plots that were used during the modelling framework. The spatial a white square within each spatial prediction map (for visualisation purposes white squares are not scaled to the plot's real size). Spatial predictions for other traits can be found in Fig. S1-S7.

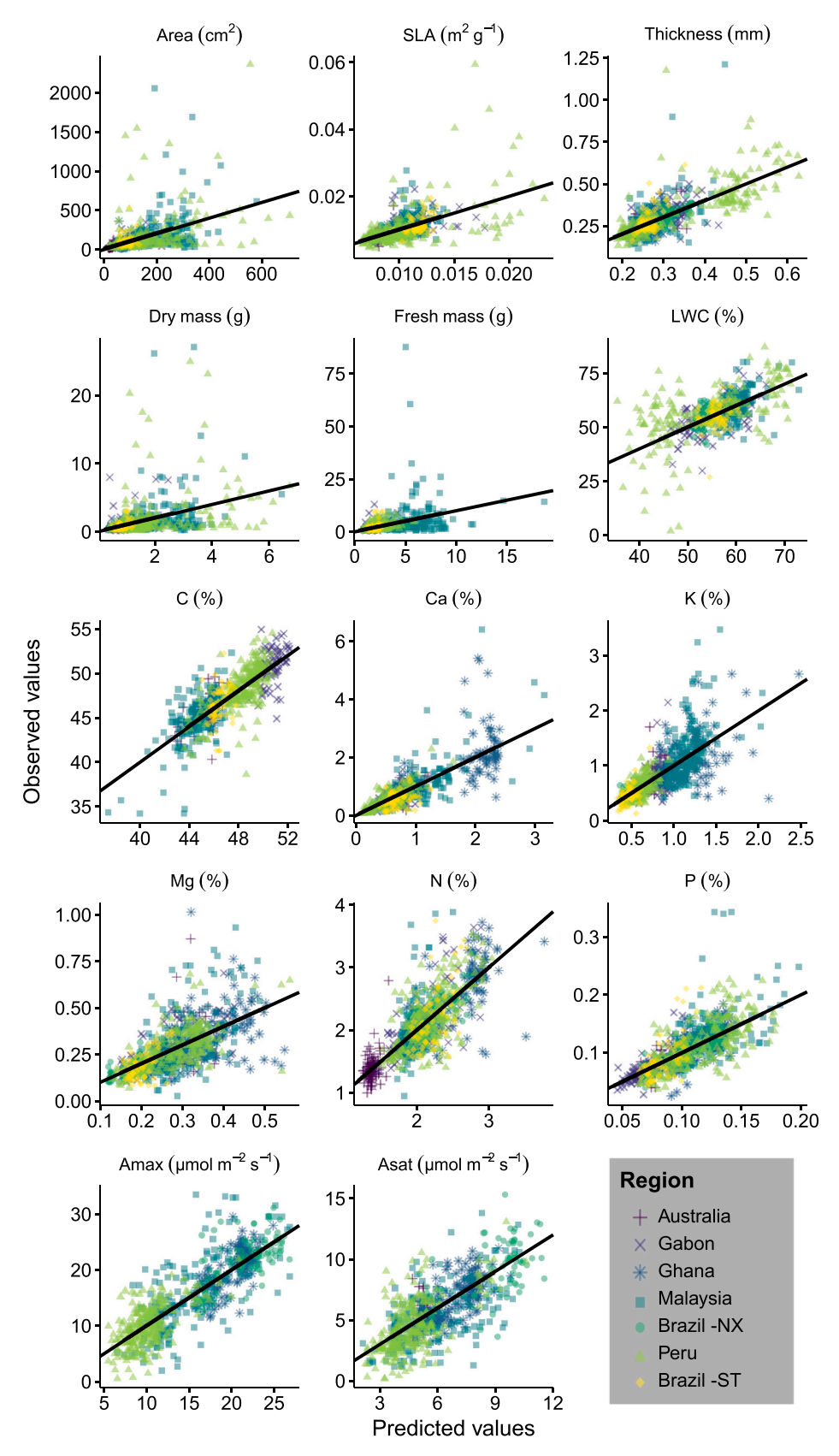


Fig. 5. Models predictions to the 20% test data from the regional models fitted with 80% of the trait data from each region across the tropics. Each colour represents an individual regional model and the coloured symbols are the observed against predicted trait values of the pixel-level $(10 \times 10 \text{ m})$ community weighted mean traits from the test dataset. The black line shows the 1:1 relationship between observed and predicted values. Model prediction accuracy is shown in Table 5. Full model results are shown in Table S5. Brazil -NX: Nova Xavantina; Brazil -ST: Santarem.

Table 5
Prediction accuracy (R^2) on the testing data among regions (shaded Region mean R^2 column) and functional traits (shaded Trait mean R^2 row). Not shaded values in the table show the prediction accuracy (R^2) on the test data per region and trait.

Location	P (%)	Amax (μmol m ⁻² s ⁻¹)	Ca (%)	N (%)	Thickness (mm)	Asat (μmol m ⁻² s ⁻¹)	Mg (%)	C (%)	SLA (m² g ⁻¹)	LWC (%)	K (%)	Dry mass (g)	Area (cm²)	Fresh mass (g)	Region mean R ²
Australia	0.21	-	0.33	0.17	0.21	0.03	0.12	0.34	0.25	-	0.06	-	0.35	-	0.21
Brazil -NX	0.68	0.42	0.49	0.52	0.66	0.52	0.46	-	0.54	0.07	0.07	0.38	0.08	0.31	0.40
Brazil -ST	0.47	-	0.15	0.30	0.42	-	0.28	0.07	0.29	0.05	0.29	0.25	0.04	0.18	0.23
Gabon	0.60	-	0.39	0.50	0.23	-	0.52	0.22	0.15	0.38	0.24	0.22	0.11	0.11	0.31
Ghana	0.47	0.49	0.53	0.52	0.22	0.36	0.15	-	0.14	-	0.23	-	0.29	-	0.34
Malaysia	0.34	0.48	0.50	0.27	0.31	0.36	0.31	0.38	0.06	0.24	0.28	0.07	0.11	0.03	0.27
Peru	0.49	0.36	0.69	0.44	0.64	0.38	0.46	0.47	0.32	0.34	0.30	0.09	0.18	0.20	0.38
Trait mean R ²	0.47	0.44	0.44	0.39	0.38	0.33	0.33	0.30	0.25	0.22	0.21	0.20	0.17	0.17	

^{-:} no data available; Brazil -NX: Nova Xavantina; Brazil -ST: Santarem.

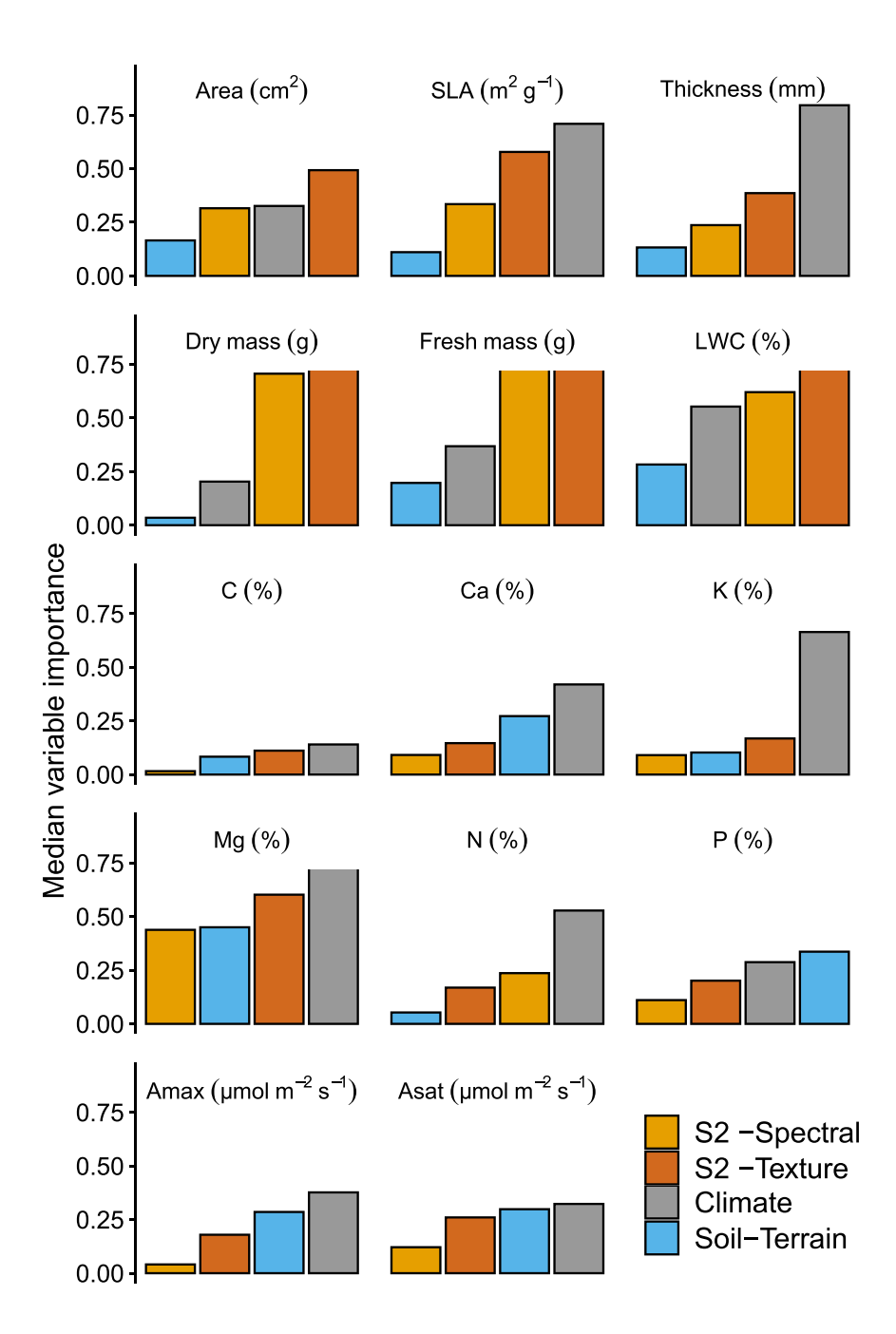


Fig. 6. Group median variable importance of spectral remote sensing, environmental and soil related variables for determining functional trait predictions in the global model. Variable importance (Y axis) ranges from 0 (no importance) to 1 (highest importance) and represents the decrease in node impurities from splitting on the variable, averaged over all trees and derived from the Out of Bag error, the resulting value has been standardised to a 0-1 scale for comparison purposes. The spectral group (S2 -Spectral) contains the select raw bands from the Sentinel-2 and the vegetation indices; Texture parameters (S2 -Texture) contain the Correlation and Entropy metrics from the grey level cooccurrence matrix obtained from the vegetation indices; Climate contains all climatic variables; Soil-Terrain contains all soil characteristics and slope. All variables are described in Table 3.

important across all traits (Fig. S9).

The local models provided a site-specific view of the most important remote sensing derived variables, environmental and soil conditions for deriving community level traits composition (Fig. S10). Sentinel-2 remote sensing related variables were more important for detecting leaf morphology and nutrient values than environmental and soil related variables in 88% of the trait models (in 75 out of 85 possible traits by region combinations). Eighty-one percent of the time (69 location by trait combinations) the canopy texture parameters were more important than the raw spectral reflectance factors. In 5.9% and 4.7% of the possible trait and region combinations, climatic or soil-topography related variables respectively were the most important for detecting community traits (Fig. S10).

4. Discussion

To the best of our knowledge, this is the first study evaluating the ability of Sentinel-2 satellite data to map plant functional traits across tropical ecosystems. Tropical forest trait mapping is fundamental for understanding of plant responses to global change, and notably the plant functional traits we predict in this study are relevant to plant species responses to a changing environment (Both et al., 2019; Nunes et al., 2019; Soudzilovskaia et al., 2013; Aguirre-Gutiérrez et al., 2019). We have demonstrated that accurate pixel-level ($10 \times 10 \, \mathrm{m}$) predictions of tropical forest functional trait distributions across the tropics can be generated by making use of extensive in-situ collected plant functional traits, geo-located canopy structure, vegetation censuses and high spectral and spatial resolution remote sensing data from the Sentinel-2 satellites.

4.1. Tropical forest trait distributions

Plant functional traits are characteristics that aid species to thrive in their environment or adapt to new conditions. Given such adaptations to specific environments it might be expected that trait variation would be higher in regions that encompass more varied environmental conditions (Enquist et al., 2015). Environmental adaptation is exemplified by the strong variation in values for most traits in Peru and Malaysia. In Peru, the data represent a climatic and altitudinal gradient ranging from the lowland Amazon in the Tambopata National Park at an elevation of 200-225 masl to plots in Acjanaco at above 3000 masl. In Malaysia, the vegetation plots are distributed across a land-use gradient ranging from undisturbed to heavily logged forests (Both et al., 2019). Environmental adaptation may be also shown by the observed differences in trait distributions between different regions across the tropics (e.g. Australia and Gabon; see also Fig. 2). The pixel-based community trait values in the Peruvian transect often extend across much of the range in trait values observed in other locations (Fig. 2). We detected an overall significant difference among locations in terms of morphological, chemical and photosynthetic traits (Table S2). This wide variation in traits suggests the presence of local biotic and abiotic controls of trait distributions and plant species adaptations that may differ among tropical regions. Such differences in trait composition highlight the importance and the challenge of sampling as fully as possible the functional trait diversity across different tropical forests. This is of pivotal importance when comparing forest responses to changing environments across multiple regions. We thus suggest that further field trait survey campaigns across the tropics are needed to improve pantropical trait predictions. As for the local biotic and abiotic controls of trait distributions, for instance, it is widely known that African tropical forests are in general less species diverse than their Asian and South American counterparts but that they have some of the highest biomass carbon storage capacity per unit area (Sullivan et al., 2017). Tropical forests in West Africa are in general drier in comparison to Amazonian tropical forests (Parmentier et al., 2007) and some African regions such as Gabon have experienced increases in temperature and decreases in precipitation over the last 30 years (Bush et al., 2020). Thus, such changes in climatic conditions as those observed in West African tropical forest may also underlie variations in species composition and the locally observed functional trait pool as shown in this study. It is also worth noting that two caveats of the community-weighted mean trait approach may account for part of the unexplained trait variation. First, it makes the assumption of a unique functional optimum in a given environment, while multiple optimal strategies – potentially corresponding to contrasting trait values – could coexist (Laughlin et al., 2018). Secondly, it does not account for the dynamic nature of communities, so that a community weighted mean at a given time point might not encompass the optimum at equilibrium (Laughlin et al., 2018).

Morphological and structural traits such as leaf area, fresh and dry mass, leaf thickness, SLA and LWC, represent trade-offs between energy acquisition, consumption and survival and form a main part of the global spectrum of plant functioning (Díaz et al., 2016). Besides investigating the predictability of such plant structural traits, we further analysed the potential for predicting leaf chemistry (C, K, Mg, Ca, N, P) and photosynthesis related traits (A_{max} and A_{sat}). Mapping chemical and photosynthetic traits at a pantropical scale has the potential for increasing our understanding of how photosynthetic capacity shifts across tropical regions and on possible impacts of a changing environment on tropical forests productivity (Guan et al., 2015; Mueller et al., 2014).

4.2. Sentinel-2 remote sensing for mapping community level trait distributions across the tropics

In their pioneering work with hyperspectral imagery and simulated multispectral Sentinel-2 data over Ghana, Laurin et al. (2016) demonstrated that Sentinel-2 imagery could be used to discriminate tropical forest types and map plant functional types. The authors argued that the full band set and vegetation indices derived from the Sentinel-2 would be advantageous for accurately mapping plant functional guilds in the tropics. By using functional trait data collected in situ across tropical forests and modelling at high spatial resolution (pixel-level) we show that most of our global trait distribution models present a high predictive power for most traits analysed, with prediction accuracy on the testing datasets being highest for predicting leaf chemical and photosynthetic capacity traits. However, we also show that the local level trait models produced less accurate predictions than the global models, probably as a result of the narrower range of plant trait values found within the region in comparison to across the regions, something also shown by Wallis et al. (2019). The prediction accuracy obtained from our models using Sentinel-2 multispectral data is similar and in some cases higher than that shown by recent studies that make use of hyperspectral imagery and other multispectral sensors to map functional traits (Martin et al., 2018; Asner et al., 2017; Asner et al., 2015). For instance our predictions on test data for leaf nitrogen, phosphorus and carbon are comparable or higher than those obtained by other innovative studies in Malaysia ($R^2 = 0.46$, 0.44 and 0.48 respectively; Martin et al., 2018), Peru ($R^2 = 0.48$, 0.39 and 0.44; Asner et al., 2015) and temperate forests ($R^2 = 0.55, 0.22, 0.46$; Nunes et al., 2017), and closely related to those obtained by Wallis et al. (2019) with other multispectral sensor for nitrogen and phosphorus ($R^2 = 0.65$ and 0.65). Specially the work of Asner et al. (2017) has shown how such plant trait predictions (with its inherent accuracies) can be used for other applications such as to guide biodiversity conservation actions. In our approach we resample the 20 m spatial resolution bands from the Sentinel-2 to 10 m pixels as to work with the highest spatial resolution available for most spectral bands. Such resampling could in principle have an effect on the match between the tree canopies' reflectance signal and the spectral signal from the Sentinel-2 pixel and could thus influence the textural parameters, by for instance, detecting lower heterogeneity.

Some of the leaf chemistry we modelled can be directly related to the reflectance obtained from the Sentinel-2 remote sensor in the visible, infrared and red-edge regions which capture the leaf biogeochemistry (Ustin and Gamon, 2010). For instance, it has been shown how carbon and carbon containing metabolites peak in reflectance at around 550 nm (band 3 in the Senitnel-2) and at the lower part of the 702-715 nm (Ely et al., 2019), which would be depicted best by the rededge band 5 in the Sentinel-2. such spectral behaviour captured by the Sentinel-2 bands contributed to the high prediction accuracy of leaf carbon in our study. Our models show how Sentinel-2 imagery, and especially the canopy texture parameters derived from it, can be especially useful for mapping traits related to leaf chemistry (Fig. 2 and Fig. S9). Moreover, our high predictive accuracy for photosynthetic capacity (Amax, Asat) is consistent with studies carried out in other vegetation types (e.g. agroecosystems; Serbin et al., 2015) where a strong association was shown between photosynthesis related traits and the red-edge spectral region. Sentinel-2 has 3 bands over the red-edge spectral region (bands 5, 6, 7) and two over the near infrared (bands 8 and 8a) with different bandwidths, which as shown by Shiklomanov et al. (2016) can be advantageous for detecting foliar nutrients such as leaf N (Schlemmer et al., 2013), as small differences in wavelength position in different bands may impact their capacity to retrieve canopy trait characteristics. Moreover, the strong relationship between photosynthetic capacity and spectral reflectance can be partly captured from the leaf N signal, as leaf N concentrations are strongly associated with photosynthetic capacity (Reich, 2012; Vincent, 2001). The N reflectance signal is often best obtained in wavebands centred between 440 and 570 nm (Ferwerda et al., 2005).

In this study we leverage evidence on covariation among traits to estimate and predict values of traits that have no clear physical effects on spectral reflectance. There is ample evidence of the existence of covariation among plant traits, as for instance between leaf N concentration, specific leaf area and leaf longevity (Walker et al., 2017). Such covariation among traits may in principle also represent covariation in the spectral reflectance patterns across vegetation types (Ma et al., 2019), especially if such individuals vary in leaf structural tissue that drive energy scattering and reflectance (Ollinger, 2011). Such covariation between traits can be helpful for mapping functional trait diversity across large spatial extents that include diverse vegetation types (Townsend et al., 2003; Both et al., 2019). We show that the spectral reflectance, image textural parameters (Entropy and Correlation), climate and soil, are highly relevant for modelling plant trait distributions across the tropics with high prediction accuracy. However, the canopy texture parameters (Entropy and Correlation) are some of the most important for attaining high trait prediction accuracies across plant functional traits (Sarker and Nichol, 2011; Wallis et al., 2019) and differences in spectral, climatic and soil conditions between different regions are key components for improving model predictions across broad spatial extents.

Image texture parameters were derived from the vegetation indices that we calculated, which in turn were derived from the raw spectral bands of the Sentinel-2. Thus, the texture metrics besides taking advantage of the high spectral resolution of the sensor also take advantage of its high spatial resolution. Although the raw spectral bands of the Sentinel-2 were not as important for predicting some functional traits as image texture, it is relevant to consider that texture values tend to differ based on the spatial resolution of the underlying data on which they are based. A larger pixel (e.g. Landsat's 30 × 30 m pixels) may thus mask differences in the landscape that could in principle be captured by the Sentinel 10×10 m resolution texture generated metrics. This therefore highlights the relevance of Sentinel-2 imagery for functional plant functional trait predictions in comparison to others with lower spectral and spatial resolution. Image texture parameters can help characterise the upper surface of the vegetation, which in our study is composed of varied sets of functional trait characteristics that confer them different spectral responses. When such spectral differences are analysed with

grey level co-occurrence matrices, the generated image texture parameters (e.g. entropy and correlation) can help differentiate contrasting vegetation in the landscape. The role of texture parameters for modelling biomass and functional traits has also been recognised by other studies focusing not only on mapping functional traits along elevation gradients but also for estimating standing biomass (Wallis et al., 2019). Moreover, such relevance of texture parameters does not seem to be limited to the spatial resolution of the Sentinel-2 imagery as shown when using high spatial resolution SPOT imagery for modelling forest aboveground biomass (Hlatshwayo et al., 2019) and WorldView-3 for tree species identification (Ferreira et al., 2019), or lower spatial resolution data as that from the Landsat (Wallis et al., 2019). Other added value of the Sentinel-2 in contrast to finer spatial resolution satellites (e.g. SPOT and WorldView-3) is its high revisit period, to obtain cloud free imagery, and it's free availability. Moreover, soil properties can be informative when modelling trait distributions across regions in the tropics as they partly drive the plant functional and species compositional turnover (Prada et al., 2017; Asner et al., 2016). In our study different vegetation plots appeared to be on soils with different parent materials resulting in varying cation exchange capacity, pH and soil texture, and thus including differences between sites contributes to increasing the prediction accuracy of trait distributions.

Although in the past it was thought not to be possible to map individual plant species or functional traits (Price, 1994; Ustin and Gamon, 2010), the advent of remotely sensed data with high spectral, spatial and temporal resolution has made it possible to extract information on the chemical and structural composition of forest canopies even in highly biodiverse tropical forests. This has been demonstrated with the use of hyperspectral sensors (Asner et al., 2017; Asner et al., 2015; Jetz et al., 2016), which often collect hundreds of spectral bands at very high spatial and spectral resolutions but at relatively small spatial extents and often without temporal replication. More research is needed to disentangle to what extent hyperspectral data offers more information to that offered by the Sentinel-2 sensors for an increased mapping accuracy of functional traits of tropical forests. As shown by Laurin et al. (2016), results obtained with simulated Sentinel-2 data are highly comparable to those obtained from hyperspectral imagery for mapping forest types, dominant tree species and functional guilds. Being able to monitor functional traits at high spatial and temporal resolution with multispectral data ranging from the visible to the shortwave infrared across the tropics and with freely available data opens new opportunities for understanding the effects of environmental changes on biodiversity at a local scale. This is because functional traits play a major role in determining ecosystem productivity and functioning, e.g. carbon capture (Díaz et al., 2019; Carmona et al., 2016). Moreover, spatially explicit models of functional traits shift across the tropics can help decipher how ecosystem functioning varies even among tropical areas, providing a cost-effective pathway to identifying regions of high conservation value and hence aid in the creation of locally adequate biodiversity conservation policies. Overall, our findings are of relevance for informing biodiversity monitoring policies under ecosystem change as we show that accurate predictions of relevant plant functional traits can be obtained in high biodiversity areas such as the tropics. Our approach thus facilitates tracking possible shifts in trait distributions and composition across large spatial extents as a response to environmental changes using the Sentinel-2 satellites.

5. Conclusions

Tropical forest ecosystems are witnessing a rapid transformation as a result of changing environmental conditions and direct human impacts (Lewis et al., 2015; Taubert et al., 2018; Aguirre-Gutiérrez et al., 2019). However, we cannot adequately understand or simulate tropical ecosystem responses to environmental changes based solely on current ecosystem model approaches as these are unable to capture the high diversity of plant ecosystem functions in the species-rich tropics.

Neglect of functional biodiversity can oversimplify the simulated response of an ecosystem to an environmental disturbance. Here we show the high variation in functional traits that exists among tropical regions, which hints at the different capabilities of such forests to respond to a changing environment. We demonstrate opportunities for measuring the distribution of key functional traits across tropical forest ecosystems at the pixel-level using the Sentinel-2 satellites, which if done across time could reveal areas where functional shifts have occurred and likely where biodiversity conservation/amelioration measures are needed. Although the Sentinel-2 satellites show high promise for this endeayour, our approach is limited by the short time interval since they were launched (i.e. 2015) and the lower spectral resolution of Sentinel-2 imagery in comparison to that derived from hyperspectral sensors. Methods and data products are needed to track changes in functional composition in forest ecosystems across time and space. We demonstrate a new approach to develop a rapid monitoring tool for capturing the effects of a changing environment across the tropics. This new tool has the potential to contribute to a more robust and evidence-based policy-making for conservation of tropical forest ecosystems.

Authorship contribution statement

J.A.G. conceived the study, designed and carried out the analysis and wrote the first draft of the paper. Y.M. conceived and implemented the GEM Network, obtained funding for most of the GEM traits field campaigns and commented on earlier versions of the manuscript. S.R. advised on statistical and remote sensing analysis and commented on earlier versions of the manuscript. All co-authors participated in or coordinated vegetation, trait data and/or soil data collection or processed field data. The authors named between S.A.B. and L.J.T.W. are listed alphabetically. All co-authors commented on and approved the manuscript.

Declaration of Competing Interest

The authors declare that they have no known competing financial interests or personal relationships that could have appeared to influence the work reported in this paper.

Acknowledgements

This work is a product of the Global Ecosystems Monitoring (GEM) network (gem.tropicalforests.ox.ac.uk). J.A.G. was funded by the Natural Environment Research Council (NERC; NE/T011084/1 and NE/S011811/1) and the Netherlands Organisation for Scientific Research (NWO) under the Rubicon programme with project number 019.162LW.010. The traits field campaign was funded by a grant to Y.M. from the European Research Council (Advanced Grant GEM-TRAIT: 321131) under the European Union's Seventh Framework Programme (FP7/2007-2013), with additional support from NERC Grant NE/D014174/1 and NE/J022616/1 for traits work in Peru, NERC Grant ECOFOR (NE/K016385/1) for traits work in Santarem, NERC Grant BALI (NE/K016369/1) for plot and traits work in Malaysia and ERC Advanced Grant T-FORCES (291585) to Phillips for traits work in Australia. Plot setup in Ghana and Gabon were funded by a NERC GrantNE/I014705/1 and by the Royal Society-Leverhulme Africa Capacity Building Programme. The Malaysia campaign was also funded by NERC GrantNE/K016253/1. Plot inventories in Peru were supported by funding from the US National Science Foundation Long-Term Research in Environmental Biology program (LTREB; DEB 1754647) and the Gordon and Betty Moore Foundation Andes-Amazon Program. Plots inventories in Nova Xavantina (Brazil) were supported by the National Council for Scientific and Technological Development (CNPq), Long Term Ecological Research Program (PELD), Proc. 441244/2016-5, and the Foundation of Research Support of Mato Grosso (FAPEMAT),

Project ReFlor, Proc. 589267/2016. During data collection, I.O. was supported by a Marie Curie Fellowship (FP7-PEOPLE-2012-IEF-327990). GEM trait data in Gabon was collected under authorisation to Y.M. and supported by the Gabon National Parks Agency. D.B. was funded by the Fondation Wiener-Anspach. W.D.K. acknowledges support from the Faculty Research Cluster 'Global Ecology' of the University of Amsterdam. M.S. was funded by a grant from the Ministry of Education, Youth and Sports of the Czech Republic (INTERTRANSFER LTT19018). Y.M. is supported by the Jackson Foundation. We thank the two anonymous reviewers and Associate Editor G. Henebry for their insightful comments that helped improved this manuscript.

Appendix A. Supplementary data

Supplementary data to this article can be found online at https://doi.org/10.1016/j.rse.2020.112122.

References

- Abatzoglou, J.T., Dobrowski, S.Z., Parks, S.A., Hegewisch, K.C., 2018. TerraClimate, a high-resolution global dataset of monthly climate and climatic water balance from 1958–2015. Sci. data 5, 170191.
- Aguirre-Gutiérrez, J., Oliveras, I., Rifai, S., Fauset, S., Adu-Bredu, S., Affum-Baffoe, K., et al., 2019. Drier tropical forests are susceptible to functional changes in response to a long-term drought. Ecol. Lett. 22, 855–865.
- Ali, A.M., Darvishzadeh, R., Skidmore, A.K., 2017. Retrieval of specific leaf area from landsat-8 surface reflectance data using statistical and physical models. IEEE J. Selected Topics Appl. Earth Obs. Remote Sens. 10, 3529–3536.
- Asner, G.P., Martin, R.E., Anderson, C.B., Knapp, D.E., 2015. Quantifying forest canopy traits: imaging spectroscopy versus field survey. Remote Sens. Environ. 158, 15–27.
- Asner, G.P., Knapp, D.E., Anderson, C.B., Martin, R.E., Vaughn, N., 2016. Large-scale climatic and geophysical controls on the leaf economics spectrum. Proc. Natl. Acad. Sci. 113. F4043–F4051.
- Asner, G.P., Martin, R.E., Knapp, D.E., Tupayachi, R., Anderson, C.B., Sinca, F., et al., 2017. Airborne laser-guided imaging spectroscopy to map forest trait diversity and guide conservation. Science 355, 385–389.
- Barnes, E.M., Clarke, T.R., Richards, S.E., Colaizzi, P.D., Haberland, J., Kostrzewski, M., et al., 2000. Coincident Detection of Crop Water Stress, Nitrogen Status and Canopy Density using Ground Based Multispectral Data. pp. 1619.
- Beer, C., Reichstein, M., Tomelleri, E., Ciais, P., Jung, M., Carvalhais, N., et al., 2010. Terrestrial gross carbon dioxide uptake: global distribution and covariation with climate. Science 329, 834–838.
- Both, S., Riutta, T., Paine, C.T., Elias, D.M., Cruz, R.S., Jain, A., et al., 2019. Logging and soil nutrients independently explain plant trait expression in tropical forests. New Phytol. 221, 1853–1865.
- Breiman, L., 2001, Random forests, Mach. Learn, 45, 5–32.
- Bush, E.R., Jeffery, K., Bunnefeld, N., Tutin, C., Musgrave, R., Moussavou, G., et al., 2020.
 Rare ground data confirm significant warming and drying in western equatorial
 Africa. PeerJ 8, e8732.
- Cadotte, M.W., Carscadden, K., Mirotchnick, N., 2011. Beyond species: functional diversity and the maintenance of ecological processes and services. J. Appl. Ecol. 48, 1079–1087.
- Carmona, C.P., de Bello, F., Mason, N.W., Lepš, J., 2016. Traits without borders: integrating functional diversity across scales. Trends Ecol. Evol. 31, 382–394.
- Chave, J., Muller-Landau, H.C., Baker, T.R., Easdale, T.A., Steege, H.t., Webb, C.O., 2006. Regional and phylogenetic variation of wood density across 2456 neotropical tree species. Ecol. Appl. 16, 2356–2367.
- Clark, M.L., 2017. Comparison of simulated hyperspectral HyspIRI and multispectral Landsat 8 and Sentinel-2 imagery for multi-seasonal, regional land-cover mapping. Remote Sens. Environ. 200, 311–325.
- Daughtry, C., Walthall, C.L., Kim, M.S., De Colstoun, E.B., McMurtrey Iii, J.E., 2000.

 Estimating corn leaf chlorophyll concentration from leaf and canopy reflectance.

 Remote Sens. Environ. 74, 229–239.
- Díaz, S., Cabido, M., 2001. Vive la différence: plant functional diversity matters to ecosystem processes. Trends Ecol. Evol. 16, 646–655.
- Díaz, S., Kattge, J., Cornelissen, J.H., Wright, I.J., Lavorel, S., Dray, S., et al., 2016. The global spectrum of plant form and function. Nature 529, 167–171.
- Díaz, S., Settele, J., Brondízio, E., Ngo, H.T., Guèze, M., Agard, J., et al., 2019. Summary for policymakers of the global assessment report on biodiversity and ecosystem services of the intergovernmental science-policy platform on biodiversity and ecosystem services. https://www.ipbes.net/sites/default/files/downloads/spm_unedited_advance_for_ posting_htm.pdf ADVANCE_UNEDITED_VERSION.
- Ely, K.S., Burnett, A.C., Lieberman-Cribbin, W., Serbin, S.P., Rogers, A., 2019.
 Spectroscopy can predict key leaf traits associated with source-sink balance and carbon-nitrogen status. J. Exp. Bot. 70, 1789–1799.
- Enquist, B.J., Norberg, J., Bonser, S.P., Violle, C., Webb, C.T., Henderson, A., et al., 2015.
 Scaling from traits to ecosystems: developing a general trait driver theory via integrating trait-based and metabolic scaling theories. In: Anonymous Advances in Ecological Research. Elsevier, pp. 249–318.

- Enquist, B.J., Bentley, L.P., Shenkin, A., Maitner, B., Savage, V., Michaletz, S., et al., 2017.
 Assessing trait-based scaling theory in tropical forests spanning a broad temperature gradient. Glob. Ecol. Biogeogr. 26, 1357–1373.
- Esquivel-Muelbert, A., Baker, T.R., Dexter, K.G., Lewis, S.L., Brienen, R.J., Feldpausch, T.R., et al., 2019. Compositional response of Amazon forests to climate change. Glob. Chang. Biol. 25, 39–56.
- Farr, T.G., Rosen, P.A., Caro, E., Crippen, R., Duren, R., Hensley, S., et al., 2007. The shuttle radar topography mission. Rev. Geophys. 45.
- Fell, M., Ogle, K., 2018. Refinement of a theoretical trait space for north American trees via environmental filtering. Ecol. Monogr. 88, 372–384.
- Ferreira, M.P., Wagner, F.H., Aragão, L.E., Shimabukuro, Y.E., & de Souza Filho, Carlos Roberto. (2019). Tree species classification in tropical forests using visible to shortwave infrared WorldView-3 images and texture analysis. ISPRS J. Photogramm. Remote Sens., 149, 119–131.
- Ferwerda, J.G., Skidmore, A.K., Mutanga, O., 2005. Nitrogen detection with hyperspectral normalized ratio indices across multiple plant species. Int. J. Remote Sens. 26, 4083–4095.
- Gallagher, R.V., Falster, D.S., Maitner, B.S., Salguero-Gómez, R., Vandvik, V., Pearse, W.D., et al., 2020. Open Science principles for accelerating trait-based science across the tree of life. Nat. Ecol. Evol. 4, 294–303.
- Georganos, S., Grippa, T., Gadiaga, A.N., Linard, C., Lennert, M., Vanhuysse, S., et al., 2019. Geographical random forests: a spatial extension of the random forest algorithm to address spatial heterogeneity in remote sensing and population modelling. Geocarto Int. 1–12.
- Grime, J.P., 1998. Benefits of plant diversity to ecosystems: immediate, filter and founder effects. J. Ecol. 86, 902-910.
- Guan, K., Pan, M., Li, H., Wolf, A., Wu, J., Medvigy, D., et al., 2015. Photosynthetic seasonality of global tropical forests constrained by hydroclimate. Nat. Geosci. 8, 284.
- Gvozdevaite, A., Oliveras, I., Domingues, T.F., Peprah, T., Boakye, M., Afriyie, L., et al., 2018. Leaf-level photosynthetic capacity dynamics in relation to soil and foliar nutrients along forest–savanna boundaries in Ghana and Brazil. Tree Physiol. 38, 1912–1925.
- Haralick, R.M., Shanmugam, K., Dinstein, I.H., 1973. Textural features for image classification. In: IEEE Transactions on Systems, Man, and Cybernetics, pp. 610–621.
- Hastie, T., Tibshirani, R., Friedman, J., 2009. The Elements of Statistical Learning, 2nd edn. York. New.
- Hawthorne, W.D., 1995. Ecological Profiles of Ghanaian Forest Trees. (Tropical forestry papers).
- Hédĺ, R., Svátek, M., Dančák, M., Rodzay, A.W., Salleh, A.B., Kamariah, A.S., 2009. A new technique for inventory of permanent plots in tropical forests: a case study from lowland dipterocarp forest in Kuala Belalong, Brunei Darussalam. Blumea-Biodiv. Evol. Biogeo. Plants 54. 124–130.
- Hengl, T., de Jesus, J.M., Heuvelink, G.B., Gonzalez, M.R., Kilibarda, M., Blagotić, A., et al., 2017. SoilGrids250m: global gridded soil information based on machine learning. PLoS One 12, e0169748.
- Hlatshwayo, S.T., Mutanga, O., Lottering, R.T., Kiala, Z., Ismail, R., 2019. Mapping forest aboveground biomass in the reforested Buffelsdraai landfill site using texture combinations computed from SPOT-6 pan-sharpened imagery. Int. J. Appl. Earth Obs. Geoinf. 74. 65–77.
- Huang, W., Ratkowsky, D.A., Hui, C., Wang, P., Su, J., Shi, P., 2019. Leaf fresh weight versus dry weight: which is better for describing the scaling relationship between leaf biomass and leaf area for broad-leaved plants? Forests 10, 256.
- Hubau, W., Lewis, S.L., Phillips, O.L., Affum-Baffoe, K., Beeckman, H., Cuní-Sanchez, A., et al., 2020. Asynchronous carbon sink saturation in African and Amazonian tropical forests. Nature 579, 80–87.
- Jetz, W., Cavender-Bares, J., Pavlick, R., Schimel, D., Davis, F.W., Asner, G.P., et al., 2016. Monitoring plant functional diversity from space. Nat. Plants 2, 16024.
- Jucker, T., Bongalov, B., Burslem, D.F., Nilus, R., Dalponte, M., Lewis, S.L., et al., 2018.
 Topography shapes the structure, composition and function of tropical forest land-scapes. Ecol. Lett. 21, 989–1000.
- Juneau, K.J., Tarasoff, C.S., 2012. Leaf area and water content changes after permanent and temporary storage. PLoS One 7, e42604.
- Kattge, Jens, et al., 2020. TRY plant trait database–enhanced coverage and open access. Global change biology 26 (1), 119–188.
- Kissling, W.D., Walls, R., Bowser, A., Jones, M.O., Kattge, J., Agosti, D., et al., 2018. Towards global data products of essential biodiversity variables on species traits. Nat. Ecol. Evol. 2, 1531–1540.
- Laughlin, D.C., Strahan, R.T., Adler, P.B., Moore, M.M., 2018. Survival rates indicate that correlations between community-weighted mean traits and environments can be unreliable estimates of the adaptive value of traits. Ecol. Lett. 21, 411–421.
- Laurin, G.V., Puletti, N., Hawthorne, W., Liesenberg, V., Corona, P., Papale, D., et al., 2016. Discrimination of tropical forest types, dominant species, and mapping of functional guilds by hyperspectral and simulated multispectral Sentinel-2 data. Remote Sens. Environ. 176, 163–176.
- Lebrija-Trejos, E., Pérez-García, E.A., Meave, J.A., Bongers, F., Poorter, L., 2010. Functional traits and environmental filtering drive community assembly in a species-rich tropical system. Ecology 91, 386–398.
- Lewis, S.L., Edwards, D.P., Galbraith, D., 2015. Increasing human dominance of tropical forests. Science 349, 827–832.
- Lortie, C.J., Brooker, R.W., Choler, P., Kikvidze, Z., Michalet, R., Pugnaire, F.L., et al., 2004. Rethinking plant community theory. Oikos 107, 433–438.
- Ma, X., Mahecha, M.D., Migliavacca, M., van der Plas, F., Benavides, R., Ratcliffe, S., et al., 2019. Inferring plant functional diversity from space: the potential of Sentinel-2. Remote Sens. Environ. 233, 111368.
- Malhi, Y., Roberts, J.T., Betts, R.A., Killeen, T.J., Li, W., Nobre, C.A., 2008. Climate

- change, deforestation, and the fate of the Amazon. Science 319, 169-172.
- Malhi, Y., Rowland, L., Aragao, L.E.O.C., Fisher, R.A., 2018. New insights into the variability of the tropical land carbon cycle from the El Nino of 2015/2016. Philos. Trans. Royal Soc. London. Series B. 373. https://doi.org/10.1098/rstb.2017.0298.
- Martin, M.E., Plourde, L.C., Ollinger, S.V., Smith, M., McNeil, B.E., 2008. A generalizable method for remote sensing of canopy nitrogen across a wide range of forest ecosystems. Remote Sens. Environ. 112, 3511–3519.
- Martin, R.E., Chadwick, K.D., Brodrick, P.G., Carranza-Jimenez, L., Vaughn, N.R., Asner, G.P., 2018. An approach for foliar trait retrieval from airborne imaging spectroscopy of tropical forests. Remote Sens. 10, 199.
- Martin, R.E., Asner, G.P., Bentley, L.P., Shenkin, A., Salinas, N., Huaypar, K.Q., et al., 2020. Covariance of sun and shade leaf traits along a tropical Forest elevation gradient. Front. Plant Sci. 10, 1810.
- McDowell, N., Allen, C.D., Anderson-Teixeira, K., Brando, P., Brienen, R., Chambers, J., et al., 2018. Drivers and mechanisms of tree mortality in moist tropical forests. New Phytol. 219, 851–869.
- Mueller, T., Dressler, G., Tucker, C., Pinzon, J., Leimgruber, P., Dubayah, R., et al., 2014.
 Human land-use practices lead to global long-term increases in photosynthetic capacity. Remote Sens. 6, 5717–5731.
- Naeem, S., Bunker, D.E., Hector, A., Loreau, M., Perrings, C., 2009. Biodiversity, Ecosystem Functioning, and Human Wellbeing: An Ecological and Economic Perspective. Oxford University Press, pp. 388.
- Navarro, L.M., Fernández, N., Guerra, C., Guralnick, R., Kissling, W.D., Londoño, M.C., et al., 2017. Monitoring biodiversity change through effective global coordination. Curr. Opin. Environ. Sustain. 29, 158–169.
- Nunes, M., Davey, M., Coomes, D., 2017. On the Challenges of Using Field Spectroscopy to Measure the Impact of Soil Type on Leaf Traits.
- Nunes, M.H., Both, S., Bongalov, B., Brelsford, C., Khoury, S., Burslem, D.F., et al., 2019. Changes in leaf functional traits of rainforest canopy trees associated with an El Niño event in Borneo. Environ. Res. Lett. 14, 085005.
- Oliver, T.H., Heard, M.S., Isaac, N.J., Roy, D.B., Procter, D., Eigenbrod, F., et al., 2015. Biodiversity and resilience of ecosystem functions. Trends Ecol. Evol. 30, 673–684.
- Oliveras, I., Bentley, L., Fyllas, N.M., Gvozdevaite, A., Shenkin, A.F., Prepah, T., et al., 2020. The influence of taxonomy and environment on leaf trait variation along tropical abiotic gradients. Front. Forests Global Change 3, 18.
- Ollinger, S.V., 2011. Sources of variability in canopy reflectance and the convergent properties of plants. New Phytol. 189, 375–394.
- Pacifici, M., Foden, W.B., Visconti, P., Watson, J.E., Butchart, S.H., Kovacs, K.M., et al., 2015. Assessing species vulnerability to climate change. Nat. Clim. Chang. 5, 215–224.
- Parmentier, I., Malhi, Y., Senterre, B., Whittaker, R.J., ATDN, Alonso, A., et al., 2007. The odd man out? Might climate explain the lower tree α-diversity of African rain forests relative to Amazonian rain forests? J. Ecol. 95. 1058–1071.
- Prada, C.M., Morris, A., Andersen, K.M., Turner, B.L., Caballero, P., Dalling, J.W., 2017. Soils and rainfall drive landscape-scale changes in the diversity and functional composition of tree communities in premontane tropical forest. J. Veg. Sci. 28, 859–870.
- Price, J.C., 1994. How unique are spectral signatures? Remote Sens. Environ. 49, 181–186.
- Qi, J., Chehbouni, A., Huete, A.R., Kerr, Y.H., Sorooshian, S., 1994. A modified soil adjusted vegetation index. Remote Sens. Environ. 48, 119–126.
- Quesada, C.A., Phillips, O.L., Schwarz, M., Czimczik, C.I., Baker, T.R., Patiño, S., et al., 2012. Basin-wide variations in Amazon forest structure and function are mediated by both soils and climate. Biogeosciences 9.
- R Development Core Team, 2014. R: A language and environment for statistical computing. R foundation for statistical computing, Vienna, Austria. ISBN 3–900051–07-0. URL. http://www.R-project.org.
- Reich, P.B., 2012. Key canopy traits drive forest productivity. Proceed. Royal Soc. B. 279, 2128–2134.
- Sarker, L.R., Nichol, J.E., 2011. Improved forest biomass estimates using ALOS AVNIR-2 texture indices. Remote Sens. Environ. 115, 968–977.
- Schlemmer, M., Gitelson, A., Schepers, J., Ferguson, R., Peng, Y., Shanahan, J., et al., 2013. Remote estimation of nitrogen and chlorophyll contents in maize at leaf and canopy levels. Int. J. Appl. Earth Obs. Geoinf. 25, 47–54.
- Schneider, F.D., Morsdorf, F., Schmid, B., Petchey, O.L., Hueni, A., Schimel, D.S., et al., 2017. Mapping functional diversity from remotely sensed morphological and physiological forest traits. Nat. Commun. 8, 1441.
- Serbin, S.P., Singh, A., Desai, A.R., Dubois, S.G., Jablonski, A.D., Kingdon, C.C., et al., 2015. Remotely estimating photosynthetic capacity, and its response to temperature, in vegetation canopies using imaging spectroscopy. Remote Sens. Environ. 167, 78–87.
- Shenkin, A., Bentley, L.P., Oliveras, I., Salinas, N., Adu-Bredu, S., Marimon, B.H., et al., 2019. The influence of ecosystem and phylogeny on tropical tree crown size and shape. BioRxiv 789255.
- Shiklomanov, A.N., Dietze, M.C., Viskari, T., Townsend, P.A., Serbin, S.P., 2016.
 Quantifying the influences of spectral resolution on uncertainty in leaf trait estimates through a Bayesian approach to RTM inversion. Remote Sens. Environ. 183, 226–238
- Soudzilovskaia, N.A., Elumeeva, T.G., Onipchenko, V.G., Shidakov, I.I., Salpagarova, F.S., Khubiev, A.B., et al., 2013. Functional traits predict relationship between plant abundance dynamic and long-term climate warming. Proc. Natl. Acad. Sci. 110, 18190, 18184
- Sullivan, M.J., Talbot, J., Lewis, S.L., Phillips, O.L., Qie, L., Begne, S.K., et al., 2017.
 Diversity and carbon storage across the tropical forest biome. Sci. Rep. 7, 39102.
- Szabó, L., Burai, P., Deák, B., Dyke, G.J., Szabó, S., 2019. Assessing the efficiency of multispectral satellite and airborne hyperspectral images for land cover mapping in

- an aquatic environment with emphasis on the water caltrop (Trapa natans). Int. J. Remote Sens. $40,\,5192-5215.$
- Taubert, F., Fischer, R., Groeneveld, J., Lehmann, S., Müller, M.S., Rödig, E., et al., 2018. Global patterns of tropical forest fragmentation. Nature 554, 519.
- Townsend, P.A., Foster, J.R., Chastain, R.A., Currie, W.S., 2003. Application of imaging spectroscopy to mapping canopy nitrogen in the forests of the central Appalachian Mountains using Hyperion and AVIRIS. IEEE Trans. Geosci. Remote Sens. 41, 1347–1354.
- Ustin, S.L., Gamon, J.A., 2010. Remote sensing of plant functional types. New Phytol. 186, 795–816.
- Van der Plas, F., Ratcliffe, S., Ruiz-Benito, P., Scherer-Lorenzen, M., Verheyen, K., Wirth, C., et al., 2018. Continental mapping of forest ecosystem functions reveals a high but unrealised potential for forest multifunctionality. Ecol. Lett. 21, 31–42.
- Vincent, G., 2001. Leaf photosynthetic capacity and nitrogen content adjustment to canopy openness in tropical forest tree seedlings. J. Trop. Ecol. 17, 495–509.
- Walker, A.P., Beckerman, A.P., Gu, L., Kattge, J., Cernusak, L.A., Domingues, T.F., et al., 2014. The relationship of leaf photosynthetic traits-Vcmax and Jmax-to leaf nitrogen, leaf phosphorus, and specific leaf area: a meta-analysis and modeling study. Ecol. Evol. 4, 3218–3235.
- Walker, A.P., McCormack, M.L., Messier, J., Myers-Smith, I.H., Wullschleger, S.D., 2017.
 Trait covariance: the functional warp of plant diversity? New Phytol. 216, 976–980.
- Wallis, C.I., Homeier, J., Peña, J., Brandl, R., Farwig, N., Bendix, J., 2019. Modeling tropical montane forest biomass, productivity and canopy traits with multispectral remote sensing data. Remote Sens. Environ. 225, 77–92.
- Wright, I.J., Reich, P.B., Westoby, M., Ackerly, D.D., Baruch, Z., Bongers, F., et al., 2004. The worldwide leaf economics spectrum. Nature 428, 821–827.